strated that HCV secretion is dependent on both apolipoprotein B (ApoB) expression and vLDL assembly in a chromosomally integrated complementary DNA (cDNA) model of HCV secretion.

These results strongly suggest that HCV might be "hitching a ride" along the lipoprotein lifecycle. Therefore, compounds previously shown to influence lipoprotein assembly and secretion could possibly exert a similar effect on HCV. To test this hypothesis, we used the full-length, RNA-based HCV full lifecycle model (JFH1/Huh7.5.1) previously shown to capture important aspects of viral replication, assembly, and infection. Using this model, we demonstrate that HCV is being actively secreted by infected cells in a Golgi-dependent pathway while bound to vLDL. Silencing ApoB messenger RNA (mRNA) by transfection with short hairpin RNA (shRNA) is shown to induce a 70% reduction in the secretion of ApoB, HCV core protein, and HCV RNA. More importantly, we find that the grapefruit flavonoid naringenin, previously shown to inhibit vLDL secretion both *in vivo* and *in vitro*, is able to reduce HCV secretion from infected cells by 80% ± 10%. We demonstrate that naringenin inhibits ApoB secretion by inhibiting the activity of the microsomal triglyceride transfer protein (MTP) as well as the transcription of 3-hydroxy-3-methyl-glutaryl-coenzyme reductase (HMGR) and acyl-coenzyme A:cholesterol acyltransferase 2 (ACAT2). Moreover, we find that naringenin is effective at a concentration of 200 μM, which is well below its toxic concentration for primary human hepatocytes and severe combined immunodeficient (SCID) mice.

Materials and Methods

Reagents and Antibodies. Fetal bovine serum (FBS), phosphate-buffered saline (PBS), Dulbecco's modified Eagle medium (DMEM), penicillin, streptomycin, and trypsin–ethylene diamine tetraacetic acid (EDTA) were obtained from Invitrogen Life Technologies (Carlsbad, CA). Lipoprotein-free FBS was purchased from Biomedical Technologies (Stoughton, MA). Insulin was obtained from Eli-Lilly (Indianapolis, IN). Oleate, naringenin, and brefeldin A were purchased from Sigma-Aldrich Chemicals (St. Louis, MO). Immunofluorescence-grade paraformaldehyde was purchased from Electron Microscope Sciences (Hatfield, PA). OptiMEM basal medium and Lipofectamine 2000 were purchased from Invitrogen Life Technologies. The SureSilencing shRNA plasmid kit for human ApoB [green fluorescent protein (GFP)] was purchased from SuperArray (Frederick, MD). An MTP fluorescent activity kit was purchased from Roar Biomedical (New York, NY). Unless otherwise noted, all other chemicals were purchased from Sigma-Aldrich Chemicals. For immunoprecipitation, Protein A-Sepharose was purchased from Invitrogen, whereas horseradish peroxidase–conjugated goat anti-mouse secondary was purchased from Santa Cruz Biotech (Santa Cruz, CA). For immunofluorescence studies, normal donkey serum and secondary F(ab')2 antibody fragments (multiple-labeling [ML] grade) were obtained from Jackson Immunoresearch (Bar Harbor, ME). Mouse anti-HCV core antigen (5 μg/mL) was purchased from US Biological (Swampscott, MA). Goat anti-ApoB (10 μg/mL) was purchased from R&D Systems, Inc. (Minneapolis, MN).

Cells and Viruses. The Huh7.5.1 human hepatoma cell line and a plasmid containing the JFH-1 genome were kindly provided by Dr. Chisari (Scripps Research Institute, La Jolla, CA) and Dr. Wakita (National Institute of Infectious Diseases, Tokyo, Japan), respectively. Huh7.5.1 cells were cultured in DMEM supplemented with 10% FBS, 200 units/mL penicillin, and 200 mg/mL streptomycin in a 5% CO_2–humidified incubator at 37°C. *In vitro* transcribed genomic JFH-1 RNA was delivered to cells by liposome-mediated transfection as described by Zhong et al.[8] Infected Huh7.5.1 cells were passaged every 3 days and used at passage <15. The presence of HCV in these cells and corresponding supernatants were determined by quantitative, reverse-transcription, polymerase chain reaction (qRT-PCR) and immunofluorescence staining. Primary human hepatocytes were purchased from BD Biosciences (San Jose, CA) and cultured on a collagen-coated 12-well plate in a C+H culture medium composed of DMEM supplemented with 10% heat-inactivated FBS, 200 U/mL penicillin/streptomycin, 7.5 μg/mL hydrocortisone, 20 ng/mL epidermal growth factor (EGF), 14 ng/mL glucagons, and 0.5 U/mL insulin. The medium was supplemented with 2% dimethyl sulfoxide for long-term culture of the primary cells.

HCV Secretion. HCV-infected Huh7.5.1 cells were plated on a 6-well plate at a density of 1×10^5 cells/cm^2 and cultured overnight in the standard medium. Prior to the beginning of the experiment, the cells were washed 3 times with PBS and cultured with DMEM containing 5% lipoprotein-free FBS. Oleate, insulin, naringenin, and brefeldin A were added at this time as described in the text. Following 24 hours of incubation, the plate was gently agitated to release mechanically bound particles, and the medium was collected, filtered to remove cellular debris, and stored at −80°C for further analysis. The attached cells were washed 3 times with PBS, harvested, pelleted, and stored at −80°C for further analysis.

Coimmunoprecipitation. The binding of Huh7.5.1-secreted JFH1 particles to ApoB was assessed with coim-

munoprecipitation. Anti-human ApoB-100 antibody (5 μg) was bound to 100 μL of Protein A-Sepharose on ice. Three milliliters of the JFH1-infected Huh7.5.1 conditioned medium (1×10^6 cells/mL) was added to the mixture, which was subsequently rotated for 4 hours at 4°C. The sample was spun down at 10,000*g* in a microcentrifuge and washed 3 times with 50 mM trishydroxymethylaminomethane (Tris)-HCl (pH 7.5) containing 5 mM EDTA. Finally, the sample was eluted in 100 μL of 10 mM Tris-HCl (pH 8.5) containing sodium dodecyl sulfate. The protein concentration in the eluted buffer was quantified as described later, and 20 μg of protein was loaded onto a 7.5% Tris-HCL resolving gel. Resolved proteins were transferred to a polyvinylidene fluoride membrane and stained against HCV core (0.5 μg/mL).

HCV Infectivity. The infectivity of the secreted HCV particles was measured as previously described.[8] Naïve Huh7.5.1 cells were grown to 80% confluence and exposed to cell culture supernatants diluted 10-fold in the culture medium. Following 1 hour of incubation at 37°C, the medium was replaced, and the cells were cultured for 3 additional days. Levels of HCV infection were determined by immunofluorescence staining for HCV core protein. The viral titer is expressed as focus forming units per milliliter of supernatant.

Human ApoB Enzyme-Linked Immunosorbent Assay (ELISA). Huh7.5.1–secreted and primary human hepatocyte–secreted ApoB was detected in the medium with the ALerCHEK, Inc. (Portland, ME), total human ApoB ELISA kit. The medium was diluted 1:10 with the specimen diluent, and the assay was carried out according to the manufacturer's directions.

HCV Core Antigen ELISA. Huh7.5.1–secreted HCV core antigen was detected in the medium with the Wako Chemicals (Cambridge, MA) ORTHO HCV antigen ELISA kit. The medium was used as is, and the assay was carried out according to the manufacturer's directions.

Total Protein Assay. The total protein content of the cells was measured with the Bio-Rad Laboratories (Hercules, CA) protein assay based on the Bardford method. Briefly, a cell pellet was lysed in 350 μL of 0.1% Triton X-100, and 5-μL samples were loaded onto a 96-well plate and incubated for 15 minutes with 250 μL of Coomassie Blue reagent at room temperature. Absorbance was measured at 595 nm and compared to a bovine serum albumin standard.

Quantitative, Real-Time, Reverse-Transcription Polymerase Chain Reaction (PCR). Virus samples collected in each experiment were filtered with a 0.45-μm filter, and a volume of 100 μL for each sample was heated at 95°C for 45 minutes. The reverse-transcription reaction step was performed on a Mastercycler epgradientS (Eppendorf) instrument using Omniscript and Sensiscript RT kits (Qiagen). Real-time PCR was performed on a Light Cycler LC-24 (Idaho Technology) using SuperScript III Platinum CellsDirect Two-Step qRT-PCR kits (Invitrogen). For the reverse-transcription step, 2 μL of a sample without RNA extraction was used. For real-time PCR, 1 μL of the reverse-transcription reactions was used. All reactions were performed according to the manufacturer's instructions with the primers detailed in Table 1.

Table 1. PCR Primers

Gene		Primer
HCV 5′ untranslated region	Forward	5′-GCAGAAAGCGTCTAGCCATGGCGT-3′
	Reverse	5′-CTCGCAAGCACCCTATCAGGCAGT-3′
MTP	Forward	5′-GAGGTTTCTCTATGCCTGTGGATTT-3′
	Reverse	5′-CCCAGGATTAACTTCTTAGCTTCCA-3′
ACAT1	Forward	5′-CAATACAATGGTGGGTGAAGAGAAG-3′
	Reverse	5′-AAAATCTTTCCTTGTTCTGGAGGTG-3′
HMGR	Forward	5′-GACCCCTTTGCTTAGATGAAAAAGA-3′
	Reverse	5′-GGACTGGAAACGGATATAAAGGTTG-3′
Actin	Forward	5′-GTCGTACCACTGGCATTGTG-3′
	Reverse	5′-CTCTCAGCTGTGGTGGTGAA-3′
ACAT2	Forward	5′-CATGCGGGAGGCTATACAAT-3′
	Reverse	5′-GTAGATGGTGCGGAAATGCT-3′

Cellular Viability. The viability of both Huh7.5.1 cells and primary human hepatocytes was studied with Thermo Fisher Scientific (Waltham, MA) Infinity aspartate aminotransferase (AST) liquid reagent. Medium samples (15 μL/well) were loaded onto a 96-well plate in triplicates and mixed with 150 μL of the AST liquid reagent. Absorbance decay was measured at the wavelength of 340 nm with 15-second intervals in a Bio-Rad Benchmark Plus spectrophotometer. Values were normalized to the total amount of AST available per culture, which was determined by total cell lysis induced by 1% Triton X-100 for 20 minutes at room temperature. Cell viability for all conditions reported in the Results section was greater than 90%.

MTP Activity Assay. MTP activity was analyzed with an MTP assay kit as previously described.[11] The assay is based on a transfer of a fluorescent signal between donor and acceptor particles due to MTP activity. Briefly, confluent Huh7.5.1 cells were stimulated with naringenin or a carrier control for 24 hours and were then washed with ice-cold PBS and scraped off the dish with a cell scraper. Samples were homogenized by sonication (3 × 5 seconds) in a buffer containing protease inhibitors. The MTP assay was performed by the incubation of 50 μg of cellular protein with 10 μL of donor and acceptor solutions in 250 μL of total buffer (15 mM Tris, pH 7.4; 40 mM NaCl; 1 mM EDTA). The in-

crease in the fluorescent signal was measured over 12 hours at 37°C at the excitation wavelength of 465 nm and emission wavelength of 538 nm.

Animal Studies. Male SCID mice (8 weeks old, 20-25 g) were obtained from Charles River Laboratories (Wilmington, MA). Animals were treated in accordance with National Institutes of Health guidelines and the Massachusetts General Hospital Subcommittee on Research Animal Care. The mice were allowed free access to laboratory chow and water *ad labium*. Naringenin was dissolved in 0.5% Tween 20 diluted in saline and given by intraperitoneal injection. Two days following the treatment, animals were sacrificed, and blood was withdrawn by cardiac puncture. AST and alanine aminotransferase (ALT) enzyme levels were assessed as described previously. Total triglycerides were measured with a kit purchased from Sigma-Aldrich Chemicals according to the manufacturer's instructions.

Silencing ApoB mRNA. HCV-infected Huh7.5.1 cells were plated in T-25 tissue culture flasks at a density of 1×10^5 cells/cm^2 and cultured overnight in the standard medium. Prior to silencing, the cells were washed 3 times with PBS, and the medium was replaced with OptiMEM basal medium. SureSilencing shRNA (GFP) plasmids against human ApoB100 as well as shRNA plasmid control (500 ng/mL) were combined with Lipofectamine 2000 in OptiMEM and incubated with the cells overnight. SureSilencing shRNA plasmids code for GFP, which was used to sort the transfected Huh7.5.1 cells with FACSAria (BD Biosciences) located at the Partners AIDS Research Center. Transfected cells (10% of the total population) were sorted directly into a 12-well plate and allowed to adhere overnight. The culture medium was conditioned by the transfected cells for 24 hours and analyzed as described previously.

Immunofluorescence Microscopy. Huh7.5.1 cells were washed 3 times with PBS and fixed in 4% electron microscopy–grade paraformaldehyde for 10 minutes at room temperature. Slides were then washed with PBS and incubated in 100 mmol/L glycine for 15 minutes to saturate reactive groups. Samples were permeabilized for 15 minutes with 0.1% Triton X-100, blocked for 30 minutes with 1% bovine serum albumin and 5% donkey serum at room temperature, and stained with primary antibodies overnight at 4°C. After additional washes with PBS, samples were stained with fluorescently tagged secondary antibodies for 45 minutes at room temperature.

Results

Huh7.5.1-Secreted HCV Is Bound to ApoB. Recent evidence suggests that HCV binds to low-density particles

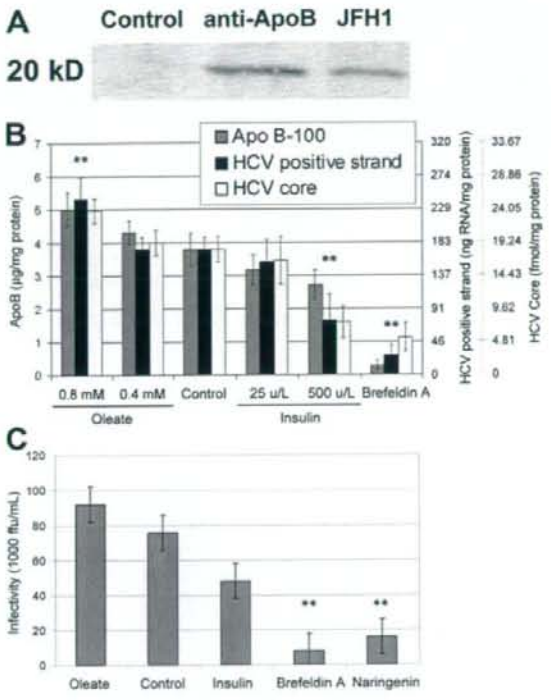

Fig. 1. (A) Immunoprecipitation of Huh7.5.1-secreted ApoB followed by anti-HCV core staining (coimmunoprecipitation). (B) Cell culture secretion of ApoB, HCV-positive strand RNA, and HCV core protein in JFH-1–infected Huh7.5.1 cells in response to oleate, insulin, and brefeldin A. The secretions of ApoB, HCV RNA, and HCV core protein are significantly up-regulated by oleate and down-regulated by insulin in a dose-dependent manner. Brefeldin A, which blocks Golgi-dependent secretion of proteins, significantly inhibits the secretion of ApoB, HCV RNA, and HCV core. Cell viability for all conditions was greater than 90%. (C) Infectivity of cell culture supernatant assessed by colony formation on naïve Huh7.5.1 cells: oleate (0.8 mM), insulin (500 U/L), brefeldin A (2.5 μg/mL), and naringenin (200 μM). $^{**}P < 0.01$.

prior to virus egress[9] and that viral secretion requires both ApoB expression and vLDL assembly to occur.[10] Therefore, HCV secreted by the JFH1/Huh7.5.1 full viral lifecycle model could potentially be secreted while bound to vLDL. To determine if Huh7.5.1-produced HCV is bound to vLDL, we immunoprecipitated the Huh7.5.1-conditioned medium against human ApoB antibodies and detected bound HCV core protein in the eluted sample. The results presented in Fig. 1A demonstrate that HCV core protein is bound to ApoB-100 in our samples. HCV core could not be detected when the sample was precipitated against irrelevant antibody (control) but was easily detected in the cell medium (JFH1).

HCV Secretion Mirrors That of vLDL. The interaction between HCV and ApoB suggests that the virus might be actively secreted by the cells while bound to vLDL. However, the interaction between these particles

might also occur outside the cell. To determine if HCV is being actively secreted by the cells while bound to vLDL, we studied viral secretion in response to oleate and insulin stimulation, which was previously shown to oppositely modulate ApoB secretion in culture.[12] Figure 1B shows ApoB, HCV core, and HCV-positive strand RNA secretion by Huh7.5.1 cells infected with the JFH-1 virus. As expected, ApoB secretion is significantly up-regulated by oleate ($P = 0.0023$, n = 5) and down-regulated by insulin ($P = 0.0073$, n = 5) in a dose-dependent manner. Similarly, HCV core protein secretion is significantly up-regulated by oleate ($P = 0.0073$, n = 3) and down-regulated by insulin ($P = 0.0223$, n = 3) in a dose-dependent manner. The secretion of HCV-positive strand RNA, measured by qRT-PCR, follows the same path. However, intracellular levels of HCV RNA remained unchanged following both treatments.

Brefeldin A is a commonly used toxin that disrupts communication between the endoplasmic reticulum and the Golgi, inhibiting the active secretion of proteins.[12,13] Not surprisingly, the addition of brefeldin A (2.5 μg/mL) blocked ApoB secretion ($P = 0.0001$, n = 5). Interestingly, brefeldin A significantly inhibits the secretion of HCV core protein ($P = 0.0021$, n = 4) and HCV-positive strand RNA ($P = 0.0006$, n = 3). To assess whether the changes in HCV core protein and RNA secretion correlate with changes of viral infectivity in the cell supernatant, we measured the ability of the secreted virus to infect naïve Huh7.5.1 cells. Figure 1C shows that the infectivity of the cell supernatant increased following oleate stimulation, decreased because of insulin, and was strongly inhibited following brefeldin A stimulation by 89% ± 10% ($P = 0.001$, n = 3). These results suggest that HCV is being actively secreted by the cells, perhaps while bound to vLDL.

HCV Core Antigen Colocalizes with ApoB. Previously, HCV core protein was shown to associate with ApoAII[4] and lipid droplets in HepG2 cells[5] overexpressing the core protein. Just recently, Huang et al.[10] demonstrated that HCV core protein colocalizes with ApoB in a chromosomally integrated cDNA model of HCV. To ascertain if HCV core protein associates with ApoB in JFH-1 virus–infected Huh7.5.1 cells, we double-stained Huh7.5.1 cells 2 days post infection by immunofluorescence for both viral and native proteins. Figure 2 demonstrates the colocalization of HCV's core and ApoB100 in infected cells. HCV core protein associates with areas in the cytoplasm that are positive to ApoB100. However, we note that although the proteins appear to be closely associated, we fail to find a one-to-one correspondence between the viral and native proteins in our model of the full viral lifecycle.

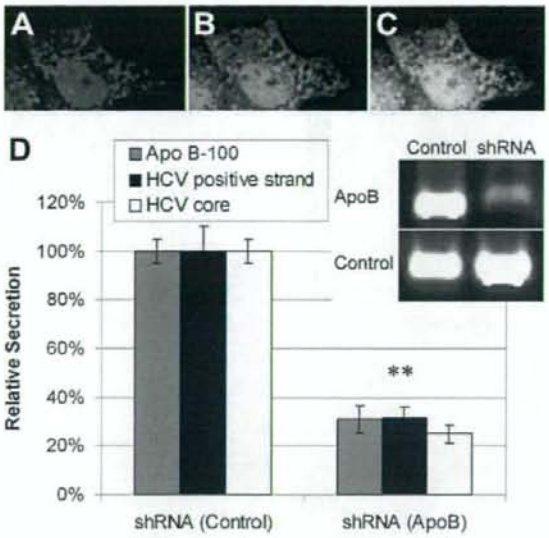

Fig. 2. Double immunofluorescence staining of JFH-1-infected Huh7.5.1 cells. (A) Staining for HCV core protein (red). (B) Staining for ApoB100 (green). (C) Superpositioning of the images demonstrates that HCV core protein associates with ApoB100 in the cytoplasm. (D) Relative secretion of ApoB, HCV-positive strand RNA, and HCV core protein in JFH-1-infected Huh7.5.1 cells following silencing of ApoB100 mRNA by SureSilencing shRNA transfection. $^{**}P < 0.01$.

The association between ApoB100 and HCV core protein as well as previous data suggests that HCV might be "tagging along" ApoB secretion. Therefore, silencing ApoB production in the cell might decrease HCV secretion. Figure 2D demonstrates a 69% ± 6% decrease in ApoB secretion following transfection with SureSilencing shRNA ($P = 0.0001$, n = 3). Interestingly, HCV core protein secretion was significantly decreased by 75% ± 4% at the same time ($P = 0.0002$, n = 3). HCV-positive strand RNA secretion was also significantly decreased by 69% ± 4% ($P = 0.0015$, n = 3).

HCV Secretion Is Inhibited by Naringenin. Naringenin is a grapefruit flavonoid previously shown to reduce cholesterol levels both *in vivo*[14] and *in vitro*.[15] It is thought that naringenin inhibits ApoB secretion by reducing the activity and expression of MTP and ACAT.[15,16] To assess if naringenin inhibits HCV secretion in a similar manner, we cultured infected Huh7.5.1 cells in the presence of naringenin for 24 hours. Figure 3A demonstrates that naringenin inhibits the secretion of HCV core ($P = 0.0001$, n = 6) and HCV-positive strand RNA ($P = 0.0006$, n = 5) in a dose-dependent manner. At the concentration of 200 μM, naringenin inhibited HCV secretion by 80% ± 10%. Interestingly, intracellular levels of HCV-positive strand RNA (Fig. 3C) as well as intracellular HCV core protein expression (Supplemen-

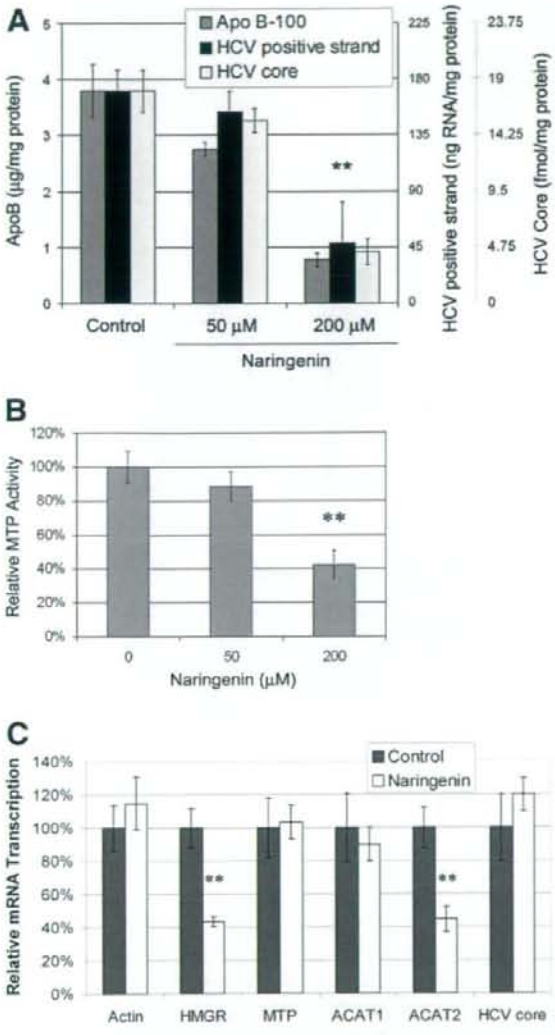

Fig. 3. (A) Inhibition of ApoB, HCV-positive strand RNA, and HCV core protein secretion by the grapefruit flavonoid naringenin. Naringenin significantly inhibits the secretion of HCV core ($P = 0.0001$, n = 6) and HCV-positive strand RNA ($P = 0.0006$, n = 5) in a dose-dependent manner. At the concentration of 200 μM, naringenin inhibited HCV secretion by 80% ± 10%. Cell viability for all conditions was greater than 90%. **$P < 0.01$. (B) Naringenin inhibits the activity of MTP in a dose-dependent manner. At the concentration of 200 μM, MTP activity was reduced by 58% ± 8% ($P = 0.0012$, n = 3). (C) Naringenin induces changes in hepatic gene transcription measured by qRT-PCR. HMGR transcription was reduced by 57% ± 3% ($P = 0.010$, n = 3), whereas the transcription of ACAT2 was reduced by 55% ± 7% ($P = 0.016$, n = 3). The mRNA levels of actin, MTP, and ACAT1 remained unchanged. Intracellular RNA levels of HCV core also remained unchanged during the 24 hours of treatment. **$P < 0.02$.

tary Fig. 1) remained unchanged. To assess whether the naringenin-induced inhibition of HCV core protein and RNA secretion correlated with changes of viral infectivity in the cell supernatant, we measured the ability of the secreted virus to infect naïve Huh7.5.1 cells. Figure 1C shows that the infectivity of the cell supernatant was strongly inhibited following naringenin stimulation by 79% ± 10% ($P = 0.0018$, n = 3).

Although the activity of naringenin has been described in uninfected cells,[15,17,18] it has yet to be characterized in HCV-infected cells. Figure 3B demonstrates that naringenin inhibits MTP activity in a dose-dependent manner. At the concentration of 200 μM, MTP activity was reduced by 58% ± 8% ($P = 0.0012$, n = 3). In addition, we demonstrate that naringenin induces significant changes in hepatic gene transcription measured by qRT-PCR (Fig. 3C). HMGR transcription was reduced by 57% ± 3% ($P = 0.010$, n = 3), whereas ACAT2 was reduced by 55% ± 7% ($P = 0.016$, n = 3). In contrast, the mRNA levels of actin, MTP, ACAT1, and HCV remained unchanged.

Naringenin Does Not Display Hepatic or* In Vivo *Toxicity. To assess the potential of naringenin-based treatment, we measured ApoB secretion in primary human hepatocytes following 24 hours of stimulation with naringenin. Figure 4A demonstrates a dose-dependent decrease in ApoB secretion following naringenin stimulation. At 200 μM naringenin, ApoB secretion was reduced by 60% ± 7% ($P = 0.007$, n = 3). The viability of primary human hepatocytes exposed to increasing concentrations of naringenin is shown in Fig. 4B. Human hepatocyte viability was 81% ± 3% at 200 μM naringenin and was not judged to be statistically different than that of the control (78% ± 3%). Human hepatocyte viability dropped significantly only at naringenin concentrations greater than 1000 μM.

To further assess naringenin potential, we delivered naringenin by intraperitoneal injection to 8-week-old male SCID mice at concentrations of 60, 300, and 1500 mg/kg (approximately 200, 1000, and 5000 μM). Animal survival was not affected by naringenin at these doses. To discern if liver damage occurred, we measured levels of AST and ALT in the animals' plasma 48 hours following injection. Figure 5 demonstrates that there was no elevation of ALT levels under all conditions. AST levels appeared to increase but remained under 100 U/L even at the highest dose. To assess naringenin's ability to reduce circulating vLDL levels, we measured total triglyceride levels in animal plasma. Figure 5A demonstrates a decrease in triglycerides following naringenin injection.

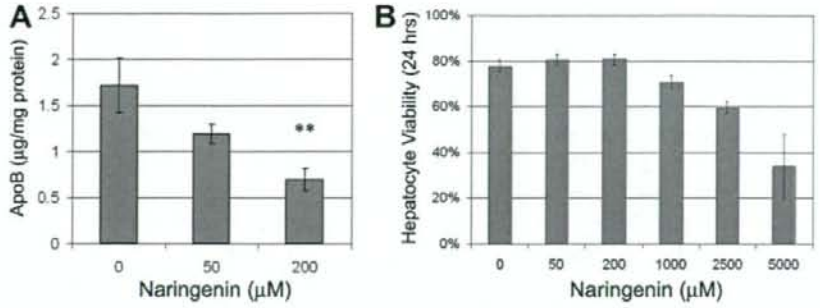

Fig. 4. (A) Naringenin stimulation inhibits ApoB secretion of primary human hepatocytes in a dose-dependent manner. At 200 µM naringenin, ApoB secretion was reduced by 60% ± 7% ($P = 0.007$, n = 3). (B) Viability of freshly isolated human hepatocytes exposed to increasing concentrations of naringenin for 24 hours. Human hepatocyte viability was 81% ± 3% at 200 µM naringenin and was not judged to be statistically different than the control (77% ± 3%). Human hepatocyte viability dropped significantly only at naringenin concentrations greater than 1000 µM.

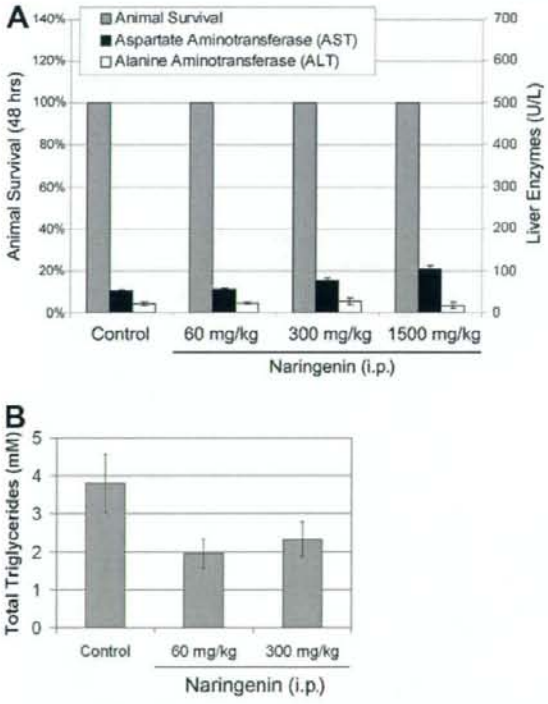

Fig. 5. Animal survival and liver enzyme release following intraperitoneal (i.p.) injection of naringenin into 8-week-old male SCID mice. Animals were injected with naringenin at 60, 300, and 1500 mg/kg of body weight. Animals were sacrificed at 48 hours, at which time liver enzymes (AST and ALT) and total triglycerides were analyzed in the animals' plasma. (A) Animal survival was monitored for several days following injection and was not affected even at the highest dose (1500 mg/kg). The ALT level appeared unchanged over all conditions, whereas AST was found to be slightly elevated at the highest dose. (B) Total triglycerides analyzed in animal plasma 24 hours following injection decreased in response to naringenin.

Discussion

HCV is a leading cause of chronic liver disease worldwide. Although the disease develops to cirrhosis in only 20% of the cases, the sheer scope of infection and lack of effective treatment make it a severe global health problem. A simulation of the US population for the years 2010-2019 predicts nearly 200,000 deaths associated with HCV infection and direct medical expenditures in excess of $10 billion. It is for these reasons that there is a pressing need for the development of alternative strategies for the treatment of HCV infection.

The interaction between HCV infection, cholesterol, and fatty acid metabolism has received significant attention, mainly because of the development of liver steatosis in chronically infected patients.[1] However, the lack of an efficient cell culture model of HCV replication and infection has significantly limited research in the field. Despite these limitations, several groups have demonstrated that HCV core protein associates with ApoAII[4] and lipid droplets in HepG2 cells[5] overexpressing the protein. The data suggest that HCV in infected patients might circulate as lipoviral particles.[19] The development of HCV replicon systems[20] has allowed for the efficient study of viral replication in culture. Using this system, Kapadia and Chisari[6] demonstrated that HCV replication is regulated by geranylgeranylation and fatty acid metabolism. Others have demonstrated that HCV nonstructural proteins, such as nonstructural protein 5A, inhibit ApoB secretion.[21]

The recent development of the JFH-1 virus[7] in combination with the Huh7.5.1 cell line[8] has allowed for the efficient infection of cells and the generation of large virus titers in culture. This model allows for the identification of intercellular infectious HCV particles with a higher density than that of their secreted counterparts,[9] suggest-

ing the binding of HCV to low-density particles in the endoplasmic reticulum. Just recently, Huang et al.[10] demonstrated that HCV assembled in ApoB and MTP enriched vesicles and that the viral secretion was dependent on both ApoB expression and vLDL assembly in a chromosomally integrated cDNA model of HCV secretion. As the association between HCV and serum β-lipoproteins (vLDL and LDL) is well known,[2] these results strongly suggest that HCV might "hitch a ride" on the lipoprotein-cholesterol lifecycle. This hypothesis is intriguing as it might explain the presence of HCV in intestinal cells, a second site of lipoprotein production.[22] In addition, it might explain HCV uptake by LDL receptor,[23,24] scavenger receptor class B type I,[25] and heparin sulfate.[26]

Our results strongly support this hypothesis. We demonstrate that HCV produced by the Huh7.5.1 cell line is bound to ApoB and that its secretion is inhibited by brefeldin A, a metabolite of the fungus *Eupenicillium brefeldianum*, which blocks the communication between the endoplasmic reticulum and the Golgi, effectively inhibiting protein secretion.[12,13] We also demonstrate that HCV secretion is up-regulated by the fatty acid oleate and down-regulated by insulin, precisely mirroring ApoB secretion by the cells.[12] Moreover, silencing ApoB100 mRNA caused a significant and parallel decrease in HCV core protein secretion. This ApoB-dependent HCV secretion pathway suggests a novel therapeutic approach for the treatment of HCV infection.

Naringin, one of the most abundant flavonoids in citrus fruits, is hydrolyzed by enterobacteria to naringenin prior to being absorbed. Naringenin has been reported to be an antioxidant,[27] MTP and ACAT inhibitor,[16] and regulator of cytochrome P4503A and 4A activity.[28,29] The ability of naringenin, or its glycosylated form, to significantly reduce plasma cholesterol levels has been demonstrated both *in vivo* and *in vitro*.[14,15] It is thought that naringenin inhibits the expression and activity of MTP, which catalyzes the transfer of lipids to the nascent ApoB molecule as it buds into the endoplasmic reticulum as a vLDL particle.[16-18] Our results demonstrate that short-term (24-hour) stimulation of infected hepatocytes with 200 μM naringenin significantly inhibits HCV secretion by 80% ± 10% and the infectivity of the titer by 79% ± 10%. At the same time, transcription of the viral RNA remains unchanged. We suggest that this is due in part to the inhibition of MTP activity by 58% ± 8% as well as the inhibition of HMGR and ACAT2 transcription. To further demonstrate naringenin as a potential therapy, we show that the compound is nontoxic to freshly isolated human hepatocytes up to concentrations greater than 1000 μM. In addition, we demonstrate that naringenin induced a 60% ± 7% decrease in ApoB secretion by primary human hepatocytes.

The concept of supplementing HCV patients' diets with naringenin is appealing. A recent clinical trial in hypercholesterolemic patients demonstrated that a low dose of naringin (400 mg/day) lowered LDL levels by 17%.[30] A similar cholesterol-lowering effect of naringenin was demonstrated in rabbits[14,31] and rats.[32] However, it is worth noting that the absorbance of naringenin through the intestinal wall is limited (less than 8%), and this suggests that short-term therapeutic doses would need to be delivered intravenously. Prior studies have suggested that the median lethal dose (50% kill) for naringenin is 2000 mg/kg for both rats and guinea pigs by intraperitoneal injection.[33] Our results show that doses up to 1500 mg/kg naringenin given by intraperitoneal injection to mice did not cause death or a marked elevation of liver enzymes, suggesting that intravenous administration of naringenin is in the realm of possibility.

The ability of the liver to regenerate in the context of the RNA-based lifecycle of HCV allows for the potential clearance of the viral infection. It is thought that clearance occurs in about 30% of HCV-infected patients. The possible reduction of HCV viral load by inhibiting viral secretion could allow uninfected cells to regenerate, potentially increasing the overall rate of viral clearance. Future studies would focus on the long-term ability of naringenin and perhaps other citrus flavonoids to reduce viral load in animal models, such as the KMT Mouse model,[34] and long-term cultures of primary human hepatocytes.

Acknowledgement: We thank Chris Pohun Chen for his help with both fluorescence-activated cell sorting and western blotting. We also thank Dr. Francis Chisari (Scripps Research Institute) for the Huh7.5.1 cell line. Microscopic imaging studies were made possible by the Core Morphology Facility of the Boston Shriners Hospital.

References

1. Guidotti LG, Chisari FV. Immunobiology and pathogenesis of viral hepatitis. Annu Rev Pathol Mech Dis 2006;1:23-61.
2. Thomssen R, Bonk S, Propfe C, Heermann KH, Kochel HG, Uy A. Association of hepatitis C virus in human sera with beta-lipoprotein. Med Microbiol Immunol 1992;181:293-300.
3. Monazahian M, Kippenberger S, Muller A, Seitz H, Bohme I, Grethe S, et al. Binding of human lipoproteins (low, very low, high density lipoproteins) to recombinant envelope proteins of hepatitis C virus. Med Microbiol Immunol 2000;188:177-184.
4. Sabile A, Perlemuter G, Bono F, Kohara K, Demaugre F, Kohara M, et al. Hepatitis C virus core protein binds to apolipoprotein AII and its secretion is modulated by fibrates. HEPATOLOGY 1999;30:1064-1076.
5. Barba G, Harper F, Harada T, Kohara M, Goulinet S, Matsuura Y, et al. Hepatitis C virus core protein shows a cytoplasmic localization and asso-

ciates to cellular lipid storage droplets. Proc Natl Acad Sci U S A 1997;94: 1200-1205.
6. Kapadia SB, Chisari FV. Hepatitis C virus RNA replication is regulated by host geranylgeranylation and fatty acids. Proc Natl Acad Sci U S A 2005; 102:2561-2566.
7. Wakita T, Pietschmann T, Kato T, Date T, Miyamoto M, Zhao Z, et al. Production of infectious hepatitis C virus in tissue culture from a cloned viral genome. Nat Med 2005;11:791-796.
8. Zhong J, Gastaminza P, Cheng G, Kapadia S, Kato T, Burton DR, et al. Robust hepatitis C virus infection in vitro. Proc Natl Acad Sci U S A 2005;102:9294-9299.
9. Gastaminza P, Kapadia SB, Chisari FV. Differential biophysical properties of infectious intracellular and secreted hepatitis C virus particles. J Virol 2006;80:11074-11081.
10. Huang H, Sun F, Owen DM, Li W, Chen Y, Gale M Jr, et al. Hepatitis C virus production by human hepatocytes dependent on assembly and secretion of very low-density lipoproteins. Proc Natl Acad Sci U S A 2007;104: 5848-5853.
11. Perlemuter G, Sabile A, Letteron P, Vona G, Topilco A, Chretien Y, et al. Hepatitis C virus core protein inhibits microsomal triglyceride transfer protein activity and very low density lipoprotein secretion: a model of viral-related steatosis. FASEB J 2002;16:185-194.
12. Dixon JL, Ginsberg HN. Regulation of hepatic secretion of apolipoprotein B-containing lipoproteins: information obtained from cultured liver cells. J Lipid Res 1993;34:167-179.
13. Misumi Y, Misumi Y, Miki K, Takatsuki A, Tamura G, Ikehara Y. Novel blockade by brefeldin A of intracellular transport of secretory proteins in cultured rat hepatocytes. J Biol Chem 1986;261:11398-11403.
14. Kurowska E, Borradaile N, Spence JD, Carroll KK. Hypocholesterolemic effects of dietary citrus juices in rabbits. Nutr Res 2000;20:121-129.
15. Allister EM, Borradaile NM, Edwards JY, Huff MW. Inhibition of microsomal triglyceride transfer protein expression and apolipoprotein B100 secretion by the citrus flavonoid naringenin and by insulin involves activation of the mitogen-activated protein kinase pathway in hepatocytes. Diabetes 2005;54:1676-1683.
16. Wilcox LJ, Borradaile NM, Dreu LED, Huff MW. Secretion of hepatocyte apoB is inhibited by the flavonoids, naringenin and hesperetin, via reduced activity and expression of ACAT2 and MTP. J Lipid Res 2001;42:725-734.
17. Borradaile NM, Dreu LED, Barrett PHR, Huff MW. Inhibition of hepatocyte apoB secretion by naringenin: enhanced rapid intracellular degradation independent of reduced microsomal cholesteryl esters. J Lipid Res 2002;43:1544-1554.
18. Borradaile NM, Dreu LED, Barrett PHR, Behrsin CD, Huff MW. Hepatocyte ApoB-containing lipoprotein secretion is decreased by the grapefruit flavonoid, naringenin, via inhibition of MTP-mediated microsomal triglyceride accumulation. Biochemistry 2003;42:1283-1291.
19. Andre P, Perlemuter G, Budkowska A, Bre'chot C, Lotteau V. Hepatitis C virus particles and lipoprotein metabolism. Semin Liver Dis 2005;25:93-104.
20. Lohmann V, Korner F, Koch J, Herian U, Theilmann L, Bartenschlager R. Replication of subgenomic hepatitis C virus RNAs in a hepatoma cell line. Science 1999;285:110-113.
21. Domitrovich AM, Felmlee DJ, Siddiqui A. Hepatitis C virus nonstructural proteins inhibit apolipoprotein B100 secretion. J Biol Chem 2005;280: 39802-39808.
22. Deforges S, Evlashev A, Perret M, Sodoyer M, Pouzol S, Scoazec JY, et al. Expression of hepatitis C virus proteins in epithelial intestinal cells in vivo. J Gen Virol 2004;85(pt 9):2515-2523.
23. Nahmias Y, Casali M, Barbe L, Berthiaume F, Yarmush ML. Liver endothelial cells promote LDL-R expression and the uptake of HCV-like particles in primary rat and human hepatocytes. HEPATOLOGY 2006;43:257-265.
24. Agnello V, Abel G, Elfahal M, Knight GB, Zhang QX. Hepatitis C virus and other flaviviridae viruses enter cells via low density lipoprotein receptor. Proc Natl Acad Sci U S A 1999;96:12766-12771.
25. Maillard P, Huby T, Andréo U, Moreau M, Chapman J, Budkowska A. The interaction of natural hepatitis C virus with human scavenger receptor SR-BI/CLA1 is mediated by ApoB containing lipoproteins. FASEB J 2006; 20:735-737.
26. Barth H, Schnober EK, Zhang F, Linhardt RJ, Depla E, Boson B, et al. Viral and cellular determinants of the hepatitis C virus envelope-heparan sulfate interaction. J Virol 2006;80:10579-10590.
27. Kanno S-I, Tomizawa A, Hiura T, Osanai Y, Shouji A, Ujibe M, et al. Inhibitory effects of naringenin on tumor growth in human cancer cell lines and sarcoma S-180-implanted mice. Biol Pharm Bull 2005;28:527-530.
28. Moon YJ, Wang X, Morris ME. Dietary flavonoids: effects on xenobiotic and carcinogen metabolism. Toxicol In Vitro 2006;20:187-210.
29. Huong DT, Takahashi Y, Ide T. Activity and mRNA levels of enzymes involved in hepatic fatty acid oxidation in mice fed citrus flavonoids. Nutrition 2006;22:546-552.
30. Jung UJ, Kim HJ, Lee JS, Lee MK, Kim HO, Park EJ, et al. Naringin supplementation lowers plasma lipids and enhances erythrocyte antioxidant enzyme activities in hypercholesterolemic subjects. Clin Nutr 2003; 22:561-568.
31. Lee C-H, Jeong T-S, Choi Y-K, Hyun B-H, Oh G-T, Kim E-H, et al. Anti-atherogenic effect of citrus flavonoids, naringin and naringenin, associated with hepatic ACAT and aortic VCAM-1 and MCP-1 in high cholesterol-fed rabbits. Biochem Biophys Res Commun 2001;284:681-688.
32. Kim S-Y, Kim H-J, Lee M-K, Jeon S-M, Do G-M, Kwon E-Y, et al. Naringin time-dependently lowers hepatic cholesterol biosynthesis and plasma cholesterol in rats fed high-fat and high-cholesterol diet. J Med Food 2006;9:582-586.
33. EKMMA8 Eksperimentalna Meditsina i Morfologiya. Vol 19. Sofia, Bulgaria: Hemus; 1980:207.
34. Mercer DF, Schiller DE, Elliott JF, Douglas DN, Hao C, Rinfret A, et al. Hepatitis C virus replication in mice with chimeric human livers. Nat Med 2001;7:927-933.

JOURNAL OF VIROLOGY, June 2008, p. 5715–5724 Vol. 82, No. 12
0022-538X/08/$08.00+0 doi:10.1128/JVI.02530-07

Critical Role of Virion-Associated Cholesterol and Sphingolipid in Hepatitis C Virus Infection▽

Hideki Aizaki,[1] Kenichi Morikawa,[1] Masayoshi Fukasawa,[2] Hiromichi Hara,[1] Yasushi Inoue,[1] Hideki Tani,[3] Kyoko Saito,[2] Masahiro Nishijima,[2] Kentaro Hanada,[2] Yoshiharu Matsuura,[3] Michael M. C. Lai,[4] Tatsuo Miyamura,[1] Takaji Wakita,[1] and Tetsuro Suzuki[1]*

Department of Virology II[1] and Department of Biochemistry and Cell Biology,[2] National Institute of Infectious Diseases, Tokyo 162-8640, and Department of Molecular Virology, Research Institute for Microbial Diseases, Osaka University, Osaka 565-0871,[3] Japan, and Department of Molecular Microbiology and Immunology, University of Southern California, Los Angeles, California 90033-1054[4]

Received 27 November 2007/Accepted 17 March 2008

In this study, we establish that cholesterol and sphingolipid associated with hepatitis C virus (HCV) particles are important for virion maturation and infectivity. In a recently developed culture system enabling study of the complete life cycle of HCV, mature virions were enriched with cholesterol as assessed by the molar ratio of cholesterol to phospholipid in virion and cell membranes. Depletion of cholesterol from the virus or hydrolysis of virion-associated sphingomyelin almost completely abolished HCV infectivity. Supplementation of cholesterol-depleted virus with exogenous cholesterol enhanced infectivity to a level equivalent to that of the untreated control. Cholesterol-depleted or sphingomyelin-hydrolyzed virus had markedly defective internalization, but no influence on cell attachment was observed. Significant portions of HCV structural proteins partitioned into cellular detergent-resistant, lipid-raft-like membranes. Combined with the observation that inhibitors of the sphingolipid biosynthetic pathway block virion production, but not RNA accumulation, in a JFH-1 isolate, our findings suggest that alteration of the lipid composition of HCV particles might be a useful approach in the design of anti-HCV therapy.

Hepatitis C virus (HCV) is recognized as a major cause of chronic liver disease, including chronic hepatitis, hepatic steatosis, cirrhosis, and hepatocellular carcinoma. It presently affects approximately 200 million people worldwide (26). HCV is an enveloped positive-strand RNA virus belonging to the *Hepacivirus* genus of the family *Flaviviridae*. Its genome of ~9.6 kb encodes a polyprotein precursor of ~3,000 residues, and the structural proteins (core, E1, and E2) reside in its N-terminal region.

Little is known about the assembly of HCV and its virion structure, because efficient production of authentic HCV particles has only recently been achieved. Nucleocapsid assembly generally involves oligomerization of the capsid protein and encapsidation of genomic RNA. This process is thought to occur upon interaction of the core protein with viral RNA, and this core-RNA interaction may induce a change from RNA replication to packaging. As with related viruses, the mature HCV virion likely consists of a nucleocapsid and an outer envelope composed of a lipid membrane and envelope proteins. Expression of the structural proteins in mammalian cells has been observed to generate virus-like particles with ultrastructural properties similar to those of HCV virions (5, 29). Packaging of these HCV-like particles into intracellular vesicles as a result of budding from the endoplasmic reticulum (ER) has also been observed (8, 34). However, HCV structural proteins are observed both in the ER and in the Golgi apparatus (45). Moreover, complex N-linked glycans have been detected on the surfaces of HCV particles isolated from patient sera, suggesting that the glycans transit through the Golgi apparatus (44). Interactions between the core and E1/E2 proteins are thought to determine viral morphology and are mediated through a cytoplasmic loop present in the polytopic form of E1 (35). Recently, we and others have identified a unique HCV genotype 2a isolate, JFH-1, that is able to replicate and produce high levels of infectious virus in culture (HCVcc) (54, 56), enabling us to investigate new aspects of the HCV life cycle.

In this study, we examine the importance of cholesterol and sphingolipid in association with the HCV membrane in virion maturation and virus infectivity. Mature HCV particles are rich in cholesterol. Cholesterol depletion or hydrolysis of sphingolipid from HCV particles results in a loss of infectivity. We further demonstrate a requirement for virion-associated cholesterol and sphingolipid for viral entry.

MATERIALS AND METHODS

Cell culture. The human hepatoma cell line Huh-7, which is permissive to HCV infection, was obtained from Francis V. Chisari (The Scripps Research Institute). Human embryonic kidney 293T cells were cultured in Dulbecco's modified Eagle medium (DMEM)–10% fetal bovine serum. Huh-7 cell lines, which carry subgenomic replicon RNA of either the JFH-1 (20) or the N (11, 17) strain, were cultured as previously described (21, 46).

Reagents. The primary antibodies used in this study were mouse monoclonal antibodies against vesicular stomatitis virus glycoprotein (VSV-G) (Sigma, St. Louis, MO), HCV E1 (54) and E2 (Biodesign International, Saco, ME), caveolin-2 (New England Biolabs, Beverly, MA), and CD81 (BD Pharmingen, Franklin Lakes, NJ), as well as rabbit polyclonal antibodies against calnexin (Stressgen, Ann Arbor, MI) and HCV core (48). ISP-1/myriocin, cholesterol, and

* Corresponding author. Mailing address: Department of Virology II, National Institute of Infectious Diseases, 1-23-1 Toyama, Shinjuku-ku, Tokyo 162-8640, Japan. Phone: 81 3 5285 1111. Fax: 81 3 5285 1161. E-mail: tesuzuki@nih.go.jp.

▽ Published ahead of print on 26 March 2008.

heparinase I were purchased from Sigma, and recombinant *Bacillus cereus* sphingomyelinase (SMase) was obtained from Higeta Shoyu (Tokyo, Japan). (1*R*,3*R*)-*N*-(3-Hydroxy-1-hydroxymethyl-3-phenylpropyl) dodecanamide (HPA-12), which was synthesized as described elsewhere (24), was a gift from Shu Kobayashi (University of Tokyo).

Plasmids. pCAE1 and pCAE2 contain HCV cDNAs spanning the E1 region (amino acids 192 to 383) with a FLAG tag at the N terminus and the E2 region (amino acids 384 to 809) with a Myc tag at the N terminus of strain NIHJ1 (1), respectively, under the control of the CAG promoter (38). pCAV340V and pCAV711V consist of the ectodomains of E1 and E2, respectively, with the N-terminal signal sequences, transmembrane domains, and cytoplasmic domains derived from VSV-G, as described elsewhere (50) (see Fig. 4D).

Virus production. Plasmid pJFH1, containing full-length cDNA of the JFH-1 isolate, was used to generate HCVcc as described elsewhere (23, 33, 34, 54). pJ6/JFH was obtained from JFH1 by replacement of the 5′ untranslated region to the p7 region (EcoRI-BclI) of J6. In vitro-transcribed RNA from linearized pJFH1 or pJ6/JFH1 was delivered to Huh-7 cells by electroporation. Culture supernatants were collected at 72 h posttransfection, clarified by low-speed centrifugation, passed through a 0.45-mm-pore-size filter, and concentrated using an Amicon Ultra-15 unit (Millipore, Bedford, MA) or by ultracentrifugation (23). Infectious titers, HCV RNA copies, and core protein concentrations of the viral stocks were $\sim 5 \times 10^3$ focus-forming units per ml, $\sim 1 \times 10^7$ copies/ml, and $\sim 1 \times 10^4$ fmol/liter, respectively. HCVcc was isolated by a combination of ultrafiltration, ion-exchange chromatography, heparin affinity chromatography, and sucrose density ultracentrifugation (33; K. Morikawa and T. Wakita, unpublished data). Pseudotyped VSV containing E1 and E2 proteins of the HCV genotype 1a isolate H77c (HCVpv) was generated as previously described (51). Briefly, 293T cells transiently expressing E1 and E2 proteins (strain H77) were infected with VSVdelG-GFP/G, in which the G envelope gene was replaced with green fluorescent protein (GFP) and pseudotyped with VSV-G.

Determination of cholesterol and phospholipid contents of HCVcc and infected cells. Cellular and viral lipids were extracted from isolated HCVcc and from uninfected and infected Huh-7 cells. Cholesterol content was determined using the cholesterol oxidase method as previously described (14). Total phospholipid content was determined using the method of Rouser et al. (42).

Cholesterol depletion and replacement. To remove cholesterol from the HCV envelope, stock samples of HCVcc were treated with *methyl*-β-cyclodextrin (B-CD) in DMEM (Sigma) supplemented with 10% fetal bovine serum (Sigma) and nonessential amino acids (Invitrogen, Carlsbad, CA) for 1 h at 37°C, followed by centrifugation at 100,000 × *g* for 3 h to form a pellet, which was resuspended in 0.5 ml of the medium. In order to replenish cholesterol, the medium of HCVcc treated with 5 mg/ml B-CD was replaced with DMEM containing various concentrations of exogenous cholesterol (Sigma) and incubated for 1 h, followed by centrifugation to form a pellet. In order to perform HCVcc infection assays, Huh-7 cells were infected with HCVcc, with or without the treatment described above, for 1 h at 37°C and then washed as described above. Viral core protein levels in the cells and in the supernatant were quantified 72 h later using an HCV core enzyme-linked immunosorbent assay (Ortho-Clinical Diagnostics, Tokyo, Japan).

SMase treatment. HCVcc was treated with SMase at various concentrations in DMEM for 1 h at 37°C and was then centrifuged at 100,000 × *g* for 3 h to form a pellet, which was resuspended in 0.5 ml of medium for the infection assays.

HCVcc binding and internalization assays. To monitor binding, cells grown in a 6-well plate were preincubated for 1 h at 4°C, after which B-CD- or SMase-treated HCVcc was bound to the cells for 1 h at 4°C. As a measure of virus internalization, following the virus binding procedure, the cells were warmed to 37°C and maintained for 2 h, after which they were treated with 0.25% trypsin for 10 min at 37°C. Huh7-25, a CD81-negative Huh-7 subclone (3), was used to ensure removal of surface-bound virus by trypsin treatment. For both the binding and internalization assays, the resulting cells, as described above, were washed with ice-cold phosphate-buffered saline, followed by lysis with TRIzol reagent (Invitrogen). Cell-associated virus was quantified by measuring the amount of HCV RNA in the cell lysate by the real-time reverse transcription-PCR method (2, 34). Cells were treated with heparinase as previously described (33).

HCV replication assay in HCVcc-infected or replicon cells. HCV subgenomic replicon cells or cells infected with HCVcc were treated with various concentrations of inhibitors for 72 h. Total RNA was isolated from replicon cells using TRIzol reagent (Invitrogen), followed by quantification of HCV RNA by real-time reverse transcription-PCR as previously described (2, 34). Levels of core protein in the culture supernatants of HCVcc-infected cells were tested as described above.

Detection of cholesterol content of HCVcc. For [^{3}H]cholesterol labeling of viruses, HCVcc-infected or uninfected cells were incubated with 50 mCi of [1α,2α-^{3}H]cholesterol in DMEM for 24 h. Culture supernatants of the cells were incubated in the presence or absence of B-CD at 5 mg/ml for 1 h at 37°C, followed by ultracentrifugation on a 60% sucrose cushion. The virus-containing fractions and corresponding fractions from an uninfected culture were lysed in the buffer containing 1% Triton X-100 (TX-100), and radioactivity was quantified by scintillation counting. Radioactivities (in counts per minute) of HCVcc samples were determined by subtracting the radioactivity of uninfected cells from that of HCVcc-infected cells.

TABLE 1. Cholesterol and phospholipid contents of HCVcc and cells

Cell type or virus	Content (nmol/mg of protein)[a]		Chol/PL ratio
	Chol	PL	
Cells			
Uninfected	105.9 ± 10.4	253.2 ± 10.6	0.42
JFH-1 infected	116.5 ± 10.0	292.0 ± 18.4	0.40
Virus			
JFH-1	43.6 ± 2.4	33.8 ± 1.8	1.29
J6/JFH-1[b]	28.7 ± 4.8	22.7 ± 2.9	1.26

[a] Data are averages of three independent measurements ± standard deviations. Chol, cholesterol; PL, phospholipids.

[b] J6/JFH1 virus was produced from the pJ6/N2X-JFH1 construct and has structural proteins from the J6CF strain.

Metabolic labeling analysis of sphingolipid content. After 2 h of incubation with [^{14}C]serine (0.5 mCi/ml) in Opti-MEM (Invitrogen), the cells were lysed with 0.1% sodium dodecyl sulfate, and total lipid was extracted with chloroform-methanol (1:2, vol/vol). The extracts were spotted onto silica gel 60 plates (Merck, Darmstadt, Germany) and chromatographed with methyl acetate–1-propanol–chloroform–methanol–0.25% KCl (25:25:25:10:9, vol/vol). Radioactive spots were quantitatively detected by BAS 2000 (Fuji Film, Japan).

Membrane flotation assay. The membrane flotation assay was performed as previously described (46).

RESULTS

Critical role of virion-associated cholesterol. A role of virion-associated cholesterol in infectivity has been demonstrated for several enveloped viruses (4). However, little is known about the role of lipids associated with the virions of flaviviruses, including HCV, and their contribution to the viral life cycle. To determine the lipid composition of mature HCV virions, we extracted total lipid from HCVcc (JFH-1 and chimeric J6/JFH-1) prepared from the culture supernatants of cells infected with HCV, as well as the total cellular membrane fractions of uninfected and infected Huh-7 cells. The cholesterol and phospholipid contents were quantified, because these are the two major lipid constituents of biological membranes. The cholesterol-to-phospholipid molar ratio, which is known as a parameter of membrane viscosity (47), was significantly higher in virus samples (1.29 and 1.26 for JFH-1 and J6/JFH-1, respectively) than in cell membrane samples (0.40 and 0.42 for JFH-1-infected and uninfected cells, respectively) (Table 1). The ratios in viral samples were similar to or greater than those in mammalian plasma membranes, where most cellular cholesterol is found. Minimal contamination of the viral samples with extracellular microvesicles likely occurred, since only a small amount of lipid was detected in a sample prepared from the culture medium of uninfected cells (data not shown). Thus, it is likely that HCV virions are enriched with cholesterol during assembly and maturation.

To investigate a potential role for the particular lipid composition of HCV particles, HCVcc was treated with

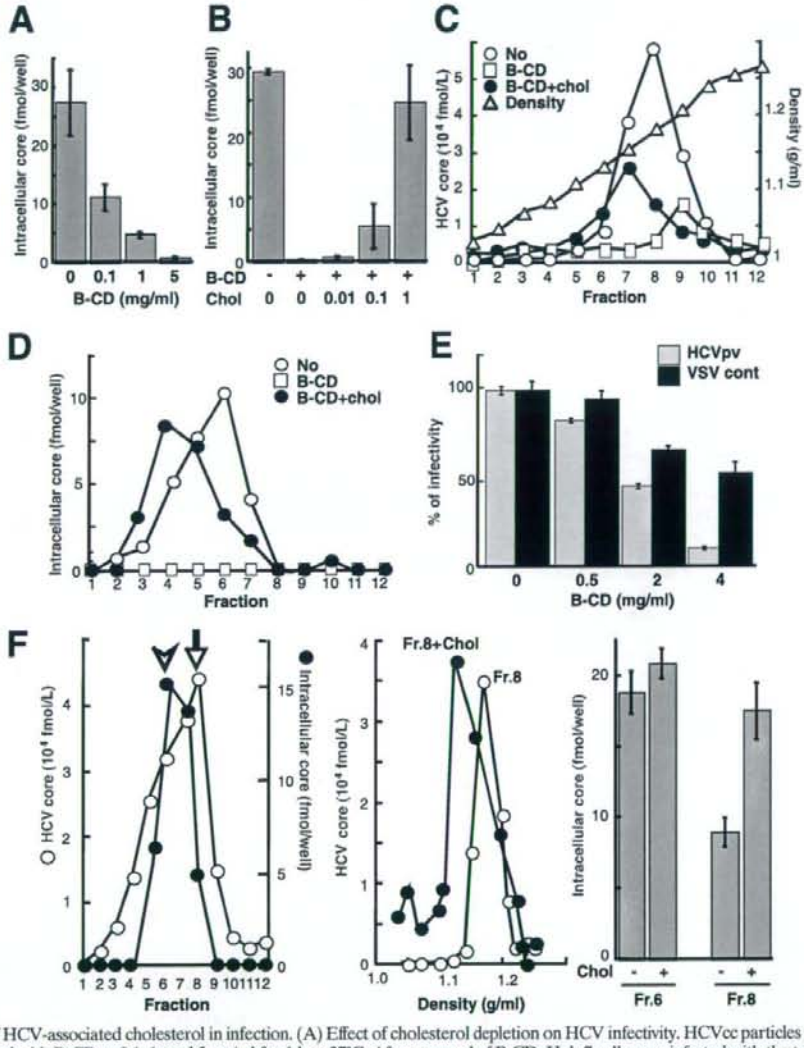

FIG. 1. Role of HCV-associated cholesterol in infection. (A) Effect of cholesterol depletion on HCV infectivity. HCVcc particles (~2 fmol of the core protein) were treated with B-CD at 0.1, 1, and 5 mg/ml for 1 h at 37°C. After removal of B-CD, Huh-7 cells were infected with the treated virus particles, after which the core protein content of infected cells at 72 h p.i. was determined as an indicator of infectivity, as previously established (24). (B) Effect of cholesterol replenishment on infectivity. After treatment with 5 mg/ml B-CD, virus was treated either with medium alone or with medium containing exogenous cholesterol for 1 h at 37°C. (C) Effect of cholesterol depletion and replenishment on density gradient profiles of the viral particles. The HCVcc treated with 5 mg/ml B-CD was replenished with exogenous cholesterol (1 mM) and then separated by 10-to-60% sucrose gradient ultracentrifugation. The core protein in each fraction was measured. The density of each fraction was determined by refractive index measurement. (D) Effects of cholesterol depletion and replenishment on viral infectivity. Each fraction (see panel C) was infected, and then the core proteins in the cells were measured at 72 h p.i. (E) Effect of cholesterol depletion on the infectivity of HCVpv (genotype 1a) (shaded bars) or the control, VSVdelG-GFP/G (solid bars). The viruses were preincubated with B-CD for 1 h at 37°C before infection. (F) (Left) The culture medium from HCVcc-producing cells was fractionated as described above. For each fraction, the amounts of core and intracellular core (infectivity) are plotted. Peaks of the core (arrow) and infectivity (arrowhead) are indicated. (Center) An aliquot of fraction 8 (peak of the core) was treated with 1 mM cholesterol for 1 h at 37°C. The resultant aliquot and an untreated aliquot of the fraction were subjected to sucrose gradient ultracentrifugation. The core in each fraction was plotted. (Right) The infectivities of fractions (Fr.) 6 and 8 (see the left panel) with or without cholesterol treatment were determined as shown above. Data are means from four independent experiments. Error bars, standard deviations.

increasing concentrations (0.1 to 5 mg/ml) of B-CD, which is known to extract cholesterol from membranes (40). The viral samples were then used to inoculate Huh-7 cells after removal of B-CD by ultracentrifugation. Infectivity was evaluated by quantifying the viral core protein in cells at 72 h postinfection (p.i.). Using an immunoassay that provides results indicative of HCV infectivity (25), we also confirmed a good correlation between the core level and

TABLE 2. Depletion of virion-associated cholesterol by B-CD

Treatment	Radioactivity (cpm) of HCVcc[a]		Avg (%[b])
	Expt 1	Expt 2	
None	5,327	5,573	5,450 (100)
B-CD (5 mg/ml)	3,643	1,646	2,644 (48.5)

[a] Determined by subtracting the radioactivity of uninfected cells from that of HCVcc-infected cells in two experiments.
[b] Percentage of the radioactivity of the untreated sample.

infectious titers (data not shown). As shown in Fig. 1A, core protein levels following B-CD treatment at 0.1, 1, or 5 mg/ml were reduced by 60, 83, or 98%, respectively, from the levels with the untreated virus. The cholesterol level of HCVcc treated with 5 mg/ml B-CD was found to be ~50% of that of untreated virions (Table 2).

To demonstrate that the reduced infection efficiency of B-CD-treated virus was caused by the reduced cholesterol content of the viral envelope, we attempted to reverse the inhibitory effect by adding exogenous cholesterol. Following treatment of HCVcc with 5 mg/ml B-CD, the drug was washed out, and increasing concentrations of cholesterol were added in an attempt to reconstitute the normal virion cholesterol content. The addition of 1 mM cholesterol completely reversed the virus infectivity (Fig. 1B). After cholesterol was replenished, the viral RNA was restored to a level similar to that in the untreated control.

To investigate the effect of cholesterol on the density of infectious HCV virions, B-CD-pretreated or untreated viral samples, as well as cholesterol-replenished treated viral samples, were subjected to sucrose density gradient centrifugation (Fig. 1C). The density of HCVcc core protein at its peak concentration in untreated virus samples was ~1.17 g/ml. When virion-associated cholesterol was removed by B-CD, the density of HCVcc core protein at its peak concentration was shifted to 1.20 g/ml. Addition of exogenous cholesterol to this cholesterol-depleted sample restored a lower-density fraction (1.15 g/ml). Figure 1D illustrates the infectivity of each gradient fraction. Untreated virus had maximum infectivity at ~1.13 g/ml (fraction 6), while, as expected, fractions from B-CD-treated viral samples exhibited minimal to no infectivity. Replenishment of depleted virus with cholesterol returned infectivity to untreated-control levels, and cholesterol-replenished virus had a buoyant density of ~1.07 g/ml (fraction 4), suggesting that HCV-associated cholesterol is crucial for viral infectivity and that the effect of a cholesterol-depleting drug is reversible. We further observed that B-CD treatment of a pseudotyped VSV containing the E1 and E2 proteins of the HCV genotype 1a isolate H77c (HCVpv) resulted in a progressive loss of infectivity, while B-CD had significantly less impact on the infectivity of the control virus VSVdelG-GFP/G (Fig. 1E).

The results described above raise the possibility that the infectivity of HCV virions with relatively low levels of incorporated cholesterol might be enhanced by supplementation with exogenous cholesterol. Density gradient fractions of culture supernatants collected from HCV-infected cells were analyzed with regard to the presence of core protein and infectivity (Fig. 1F, left). As indicated above, maximum infectivity was obtained with fraction 6 (1.13 g/ml). In contrast, a major fraction of core protein banded at a higher density (1.17 g/ml) in fraction 8. We hypothesized that fraction 8 contains lipids at lower levels than those in fraction 6. However, quantification of lipids, including cholesterol, in the fractions obtained failed, presumably due to a low sensitivity of detection. Thus, to extend our findings on the involvement of cholesterol, we added exogenous cholesterol to fraction 8, followed by ultrafiltration to remove unincorporated cholesterol. A subsequent density gradient profile demonstrated a shift in the core protein peak to 1.13 g/ml (Fig. 1F, center). A concomitant increase in the infectivity of the fraction, approaching that of untreated fraction 6, was observed (Fig. 1F, right). In contrast, supplementation of fraction 6 with exogenous cholesterol did not alter its infectivity (Fig. 1F, right) or change its density gradient (data not shown). These results suggest that exogenous cholesterol supplementation can reverse deficits in the infectivity of HCV virions due to low cholesterol content.

Sphingolipid dependence of HCV infectivity. In addition to cholesterol, sphingolipid is a major component of eukaryotic lipid membranes. We therefore investigated the functional significance of sphingomyelin (SM), the most abundant sphingolipid, with regard to HCV infectivity. HCVcc was treated for 1 h with increasing concentrations (0.1 to 10 U/ml) of bacterial SMase, which is known to hydrolyze membrane-bound SM to ceramide. Following ultracentrifugation to remove the SMase, Huh-7 cells were inoculated with the HCVcc. The amount of HCV core protein within the cells was quantified at 72 h p.i. Figure 2A shows 50 and 90% reductions in HCV infectivity after incubation of the virion with 0.1 and 1 U/ml SMase, respectively. We further observed that SMase treatment of HCVpv resulted in a progressive loss of infectivity, while SMase had no effect on the infectivity of the control virus (Fig. 2B). This demonstrates that sphingolipid, like cholesterol, plays an essential role in HCV infectivity.

Requirement for virion-associated cholesterol and sphingolipid during HCV cell entry. These findings support the idea that virion-associated cholesterol and sphingolipid may influence viral entry into host cells by altering the interaction between viral particles and a host cell factor(s). Viral entry is a multistep process including binding of the virion to the cell surface and internalization into the cytoplasm by endocytosis. To examine whether virion-associated cholesterol and SM might play a role in cell binding or postbinding events during viral entry, we used a binding assay in which Huh-7 cells preincubated for 1 h at 4°C were infected with B-CD- or SMase-treated HCVcc. Total RNA was extracted after a 1-h addition of the virions at 4°C, followed by quantification of HCV RNA. As shown in Fig. 3A, treatment of the virions with either B-CD or SMase had little influence on their ability to bind to cells.

It has been shown that CD81 plays an important role in HCV internalization but is not correlated with viral attachment (7, 33). An anti-CD81 antibody was used as a negative control for reduced viral attachment. It is likely that heparan sulfate proteoglycan on the target cell surface is needed for the initial attachment of HCV (33). Thus, heparinase I was used as a positive control for reduced HCV attachment to the cells. To examine the roles of cholesterol and sphingolipid on the HCVcc membrane in viral internalization, a virus-cell mixture

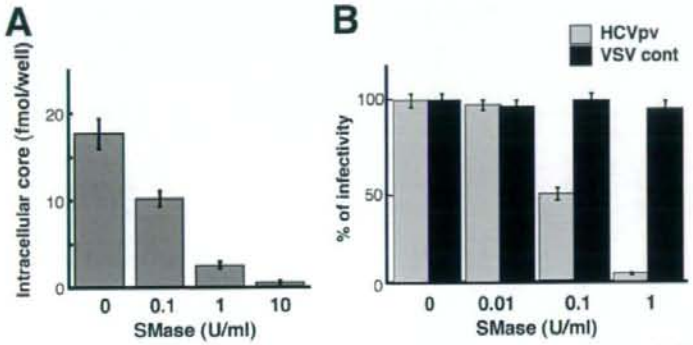

FIG. 2. Effect of SM hydrolysis on viral infectivity. (A) Effect on the infectivity of HCVcc. HCVcc was treated with 0.1, 1, or 10 U/ml SMase for 1 h at 37°C, after which SMase was removed by ultracentifugation. Huh-7 cells were infected with the treated virus, and the core protein content of infected cells was determined at 72 h p.i. (B) Effect on the infectivity of HCVpv (genotype 1a) (shaded bars) or the control, VSVdelG-GFP/G (VSV cont) (solid bars). The viruses were preincubated with SMase for 1 h at 37°C before infection. Data are means from four independent experiments. Error bars, standard deviations.

prepared at 4°C as described above was incubated for 2 h at 37°C, followed by trypsinization to remove virions that were surface bound but not internalized (Fig. 3B). We verified that 94% of surface-bound-viruses were removed by trypsinization using CD81-negative Huh-7 subclones. A marked reduction in viral RNA levels within cells was detected after pretreatment of the virus with either B-CD or SMase. These results strongly suggest that virion-associated cholesterol and sphingolipid function as key determinants of internalization but not of cell attachment.

Association of HCV structural proteins with lipid rafts. Cholesterol and sphingolipid are major components of lipid rafts, which can be isolated as detergent-resistant membranes (DRMs) by treatment with cold TX-100, followed by equilibrium flotation centrifugation. Matto et al. (30) reported that HCV core protein is associated with DRMs in cells carrying the full-length HCV replicon. To investigate whether HCV structural proteins are associated with DRMs in HCVcc-producing cells, lysates from cells infected with HCVcc were subjected to membrane flotation analysis. In the absence of detergent treatment, the majority of the core (Fig. 4A) and E1 (Fig. 4B) proteins were detected in the membrane fractions. After treatment with cold TX-100, significant amounts of both viral proteins were recovered from the DRM fraction. However, after treatment with TX-100 at 37°C, the majority of the E1 and core proteins had shifted to the detergent-soluble fractions. We also found that HCV genotype 1b E1 and E2 can be associated with the lipid raft in 293T cells transfected with an E1 or E2 expression plasmid (Fig. 4C) and that the cytoplasmic tails of envelope

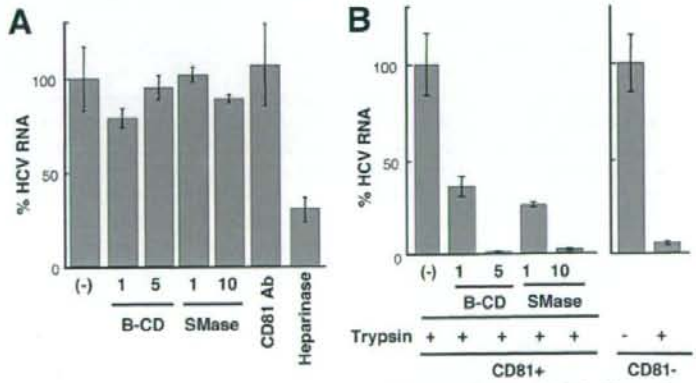

FIG. 3. Effects of B-CD or SMase on virus attachment and internalization. (A) Virus attachment to Huh-7 cells was determined at 4°C after treatment of HCVcc with B-CD (1 or 5 mg/ml) or SMase (1 or 10 U/ml). An antibody (Ab) against CD81 was used, in order to ensure that the antibody did not inhibit HCVcc binding (7, 33). Heparinase was used to reduce HCV attachment to the cell. Viral RNA copies were normalized to total cellular RNA, and the normalized RNA copies in the mock-treated sample (−) were arbitrarily set at 100%. (B) Virus internalization was measured in Huh7-25, a CD81-negative subclone ($CD81^-$) (3), and Huh7-25-CD81, which stably expresses CD81 ($CD81^+$), after treatment of the virions with B-CD or SMase. After internalization for 2 h at 37°C, cells were exposed to trypsin (trypsin +) or phosphate-buffered saline (trypsin −). Huh7-25 was used to ensure that surface-bound virus would be removed by trypsin treatment. The amounts of HCV RNA in Huh7-25 and Huh7-25-CD81 cells infected with untreated HCVcc were assigned the arbitrary value of 100%, respectively. Results are representative of four independent experiments.

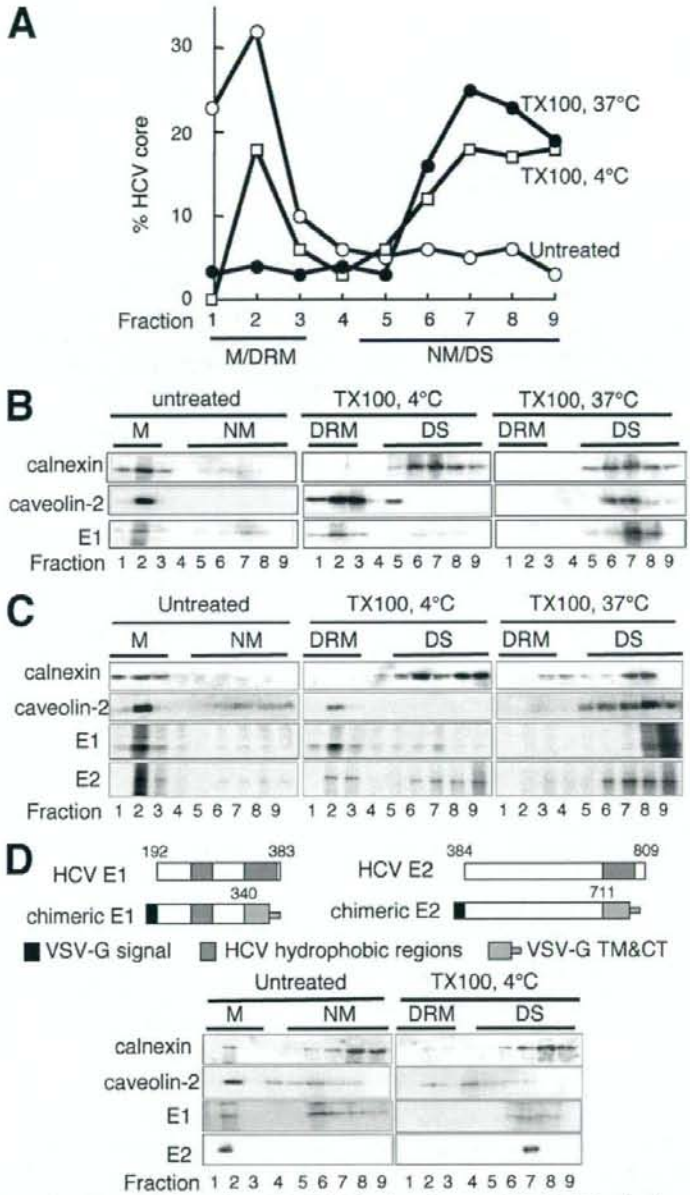

FIG. 4. Compartmentation of HCV structural proteins within DRM fractions. Lysates of HCVcc-infected cells were either treated with 1% TX-100, either on ice or at 37°C, or left untreated, followed by sucrose gradient centrifugation. (A and B) For each fraction, the amount of core protein was determined by an enzyme-linked immunosorbent assay (A), and E1, calnexin, and caveolin-2 were analyzed by Western blotting (B). The amount of core protein in each lysate (TX-100, 37°C; TX-100, 4°C; Untreated) was assigned the arbitrary value of 100%. M, membrane; NM, nonmembrane; DS, detergent soluble. (C) Lysates of 293T cells expressing HCV E1 or E2 protein were either treated with 1% TX-100, either on ice or at 37°C, or left untreated, followed by discontinuous sucrose gradient centrifugation. Each fraction was concentrated in a Centricon YM-30 filter unit and subjected to 12.5% sodium dodecyl sulfate-polyacrylamide gel electrophoresis, followed by immunoblotting with antibodies against calnexin, caveolin-2, Myc (E1), or FLAG (E2). (D) (Top) Structures of HCV envelope genes used. Amino acid positions of HCV are indicated. Signal sequence, transmembrane (TM), and cytoplasmic tail (CT) domains of VSV G protein are shown. (Bottom) Cell lysates expressing chimeric HCV E1 or E2 protein were treated with 1% TX-100 on ice or left untreated, followed by discontinuous sucrose gradient centrifugation. It has been reported that VSV-G is not associated with lipid (39). Calnexin, caveolin-2, and chimeric glycoproteins (chimeric E1 and chimeric E2) were analyzed by immunoblotting. Fractions are numbered from 1 to 9 in order from top to bottom (light to heavy).

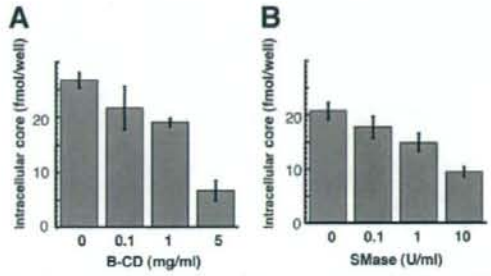

FIG. 5. Effects of B-CD or SMase treatment of cells on HCV infectivity. Huh-7 cells were either left untreated or treated with B-CD at 0.1, 1, or 5 mg/ml (A) or with SMase at 0.1, 1, or 10 U/ml (B) prior to HCVcc infection. Intracellular core levels were quantitated 72 h p.i. Data are means from four independent experiments. Error bars, standard deviations.

proteins are important for their interaction (Fig. 4D). These data suggest that subpopulations of HCV structural proteins are associated with lipid rafts in cells generating the HCV particles.

Moderate inhibition of HCV infection by B-CD or SMase treatment of host cells. It has recently been reported that cholesterol depletion or SM hydrolysis from the host cell membrane decreases HCV infection, in part by decreasing the level of CD81 on the cell surface (19, 53). The involvement of the lipid environment of the host cell plasma membrane in HCV infection was investigated in our HCVcc infection system. Prior to infection, Huh-7 cells were treated with B-CD or SMase and then washed with the medium five times. Cholesterol depletion from Huh-7 cells by B-CD at 1 or 5 mg/ml inhibited HCV core levels by 20 and 75%, respectively, compared to levels in untreated cells (Fig. 5A). We also found that hydrolysis of SM by SMase at 1 or 10 U/ml on the cells, respectively, led to moderate reduction of the viral infection, by 20 or 55% of the infection level of the untreated control (Fig. 5B). There was no influence on cell viability under the conditions of these treatments (data not shown). These findings, compared with the results in Fig. 1A and 2A, suggest that the raft-like environment on the plasma membrane likely serves as a portal for HCV entry, but HCV virion-associated cholesterol and sphingolipid more readily play more critical roles in viral infection.

Inhibitors of the sphingolipid biosynthetic pathway suppress the production of HCVcc, but not RNA replication, for a JFH-1-derived replicon. In the course of studying the involvement of lipid metabolism in the HCV life cycle, we observed that inhibitors of the sphingolipid biosynthetic pathway, including ISP-1 and HPA-12, which specifically inhibit serine palmitoyltransferase (31) and ceramide trafficking from the ER to the Golgi apparatus (55), influenced subgenomic replicons derived from the HCV-N isolate (genotype 1b), but not those derived from JFH-1. A dose-dependent decrease in HCV RNA copy numbers among HCV-N replicon cells was observed upon exposure to ISP-1 or HPA-12, as previously reported (43, 52). In contrast, these compounds had little or no effect on viral RNA accumulation in JFH-1 replicon cells (Fig. 6A). Furthermore, these compounds did not affect luciferase activity in the lysates of Huh-7 cells transfected with an in vitro-transcribed JFH-1 replicon RNA containing a luciferase reporter gene (22) (data not shown). Figure 6B shows the effects of ISP-1 and HPA-12 on de novo sphingolipid biosynthesis by replicon cells. No differences in the inhibitory effects of each compound were observed in replicon cells derived from HCV-N versus JFH-1. When de novo synthesis of sphingolipids was examined by metabolic labeling with [^{14}C]serine, ISP-1 almost completely inhibited the production of both ceramide and SM, while HPA-12 greatly inhibited the synthesis of SM but not ceramide. Levels of phosphatidylethanolamine and phosphatidylserine, into which serine is incorporated by a pathway distinct from that of sphingolipid biosynthesis, were not influenced by these drugs. These results suggest that suppression of HCV RNA replication by inhibitors of sphingolipid biosynthesis might be dependent on the viral genotype or isolate.

This observation prompted us to investigate whether inhibitors of the sphingolipid biosynthetic pathway might have the ability to prevent HCV virion production. Interestingly, when Huh-7 cells producing JFH-1 HCVcc were treated with ISP-1 or HPA-12 under conditions similar to those the replicon cells, viral core levels in the culture supernatants were greatly reduced in a dose-dependent manner. For example, exposure to 10 μM ISP-1 or 1 μM HPA-12 reduced viral core protein levels more than 85% from those for control cells (Fig. 6C). The 50% inhibitory concentrations of both drugs were less than 0.1 μM, 50-fold less than those obtained for the RNA replication of the HCV-N-replicon. Together, these results suggest that the sphingolipid biosynthetic pathway plays an important role in the production of HCV particles, but not in genome replication, in JFH-1-based HCVcc.

DISCUSSION

In this study, we demonstrated the role of HCV virion-associated cholesterol and sphingolipid in viral infectivity. Although dependence on virion-associated cholesterol for virus entry has been shown for a number of viruses (4, 6, 28, 49), this is the first study to demonstrate the importance of envelope cholesterol in a virus belonging to the family *Flaviviridae*. Furthermore, to our knowledge, the functional role of virion membrane-associated SM has not been examined in viruses. Our previous studies using Chinese hamster ovary cell mutants deficient in SM synthesis have demonstrated that reduction of cellular SM levels enhances cellular cholesterol efflux in the presence of B-CD (9, 12). Thus, it may be possible that SM plays a role in the retention of cholesterol on HCV particles due to interaction between cholesterol and SM. The finding that B-CD or SMase treatment of HCVcc markedly inhibited virus internalization but not cell attachment (Fig. 3) suggests that HCV membrane-associated cholesterol and sphingolipid are crucial for the interaction of viral glycoproteins with the virus-receptor/coreceptor required for cell entry. Cholesterol depletion or sphingolipid hydrolysis might induce a conformational change in the viral envelope, resulting in instability of the virion structure. Since the cholesterol/phospholipid ratios of membranes affect bilayer fluidity, the maturation of viral envelopes with high cholesterol/phospholipid ratios via association with rafts may be important for the stability of HCV

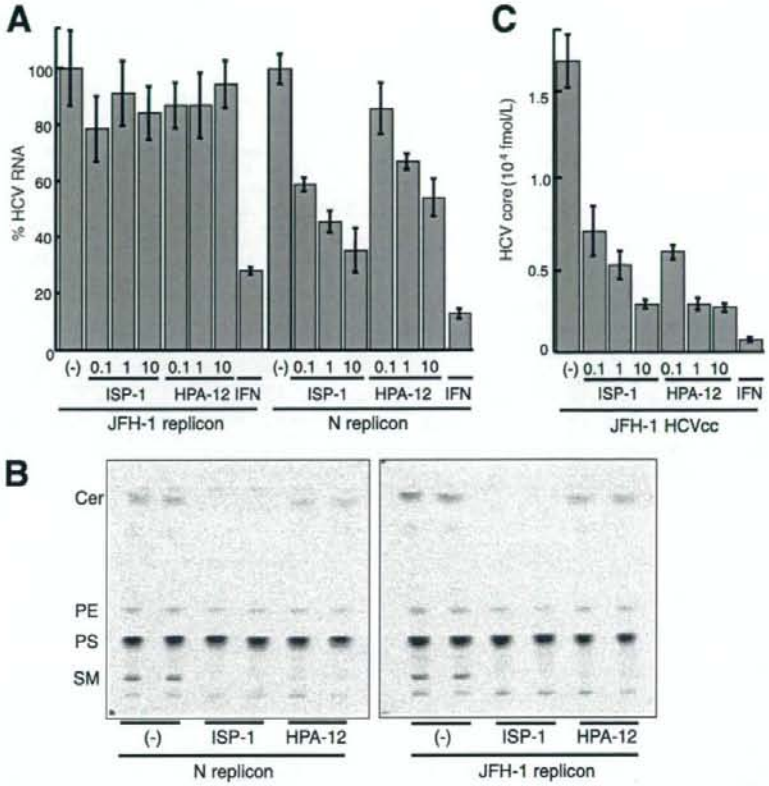

FIG. 6. Anti-HCV effects of inhibitors of the sphingolipid biosynthetic pathway. Subgenomic replicon cells derived from HCV isolate N or JFH-1, as well as HCVcc-producing cells, were treated with ISP-1 (0.1, 1, or 10 μM), HPA-12 (0.1, 1, or 10 μM) or alpha interferon (IFN) (100 U/ml) for 72 h. HCV RNA titers in the replicon cells (A) and the HCV core protein content of the culture medium of infected cells (C) were determined. Data are means from four independent experiments. Error bars, standard deviations. (B) De novo synthesis of sphingolipid in the absence or presence of ISP-1 (10 μM) and HPA-12 (10 μM) was monitored in duplicate by metabolic labeling with [^{14}C]serine for 2 h at 37°C. Cer, ceramide; PE, phosphatidylethanolamine; PS, phosphatidylserine.

particles. Replenishing the viral membrane with cholesterol following treatment with 5 mg/ml B-CD successfully restored viral infectivity to the same level as that of untreated virus (Fig. 1), suggesting that reversible B-CD-induced changes in HCV structure might critically influence viral infectivity. However, we were unable to restore viral infectivity by replenishing cholesterol after pretreatment of the virion with concentrations of B-CD exceeding 10 mg/ml (data not shown). Under these conditions, it is likely that large holes in the viral membrane destroy the virus, a result that cannot be reversed by supplying exogenous cholesterol.

How are cholesterol and sphingolipid involved in the HCV virion during the process of virus maturation? Like most positive-stranded RNA viruses, HCV is thought to assemble at the ER membrane. However, Miyanari et al. (32) reported that lipid droplets are important for HCVcc formation. These authors have shown that the characteristics of lipid-droplet-associated membranes in Huh-7 cells differ from those of ER membranes. In the case of flaviviruses, for which the mechanism of viral assembly and budding remains unclear (15), a few studies have demonstrated budding at the plasma membrane (13, 36, 37, 41), and it has been proposed that the site of budding may be virus and cell type dependent (27). We demonstrate here that subpopulations of HCV structural proteins partition into cellular detergent-resistant, lipid-raft-like membrane fractions in HCVcc-producing cells (Fig. 4) and that inhibitors of the sphingolipid biosynthetic pathway block HCV virion production (Fig. 6). Furthermore, a large proportion of HCV E2 protein incorporated into HCVcc is endoglycosidase H resistant (data not shown). Thus, membrane compartments containing cholesterol- and sphingolipid-rich microdomains may be involved in HCV virion maturation. Another explanation for the recruitment of these lipids to the HCV membrane may be an association between the virus and very-low-density lipoprotein (VLDL) or low-density lipoprotein. Recently, Huang et al. (16) demonstrated a close link between HCV production and VLDL assembly, suggesting that an HCV-VLDL complex is generated and secreted from cells.

Recent reports have demonstrated that CD81-mediated HCV infection is partly dependent on cell membrane choles-

terol (19) and SM (53). We further characterized the role of lipid on the plasma membrane in viral infectivity and found that cholesterol depletion by B-CD, as well as hydrolysis of SM by SMase, moderately inhibits HCV infectivity (Fig. 5). These results suggest that cholesterol and sphingolipid in the plasma membrane environment may assist HCV entry, while HCV virion-associated cholesterol and sphingolipid appear to play critical roles in viral infection.

We previously demonstrated that HCV RNA and nonstructural proteins are present in DRM structures, likely in the context of a lipid-raft structure, and that viral RNA is likely synthesized at a raft membrane structure in cells containing the genotype 1b HCV replicon (2, 10, 46). Here we observed that ISP-1 and HPA-12 suppress HCVcc production, but not viral RNA replication, by the JFH-1 replicon (Fig. 6). Impairment of particle assembly and maturation, rather than suppression of genome replication, by these drugs may account for the inhibition of HCV production in the JFH-1 system. Viral RNA replication of the HCV-N replicon, however, was efficiently inhibited by these compounds, as found in previous reports (43). The virus strain specificity of the anti-HCV activity of cyclosporine has recently been demonstrated: JFH-1 replication is less sensitive to cyclosporine than replication of genotype 1b strains. Furthermore, the requirement for interaction with a cellular replication cofactor, cyclophilin B, differs among HCV strains (18). It appears that ISP-1 and HPA-12 are further examples of diverse effects on HCV strain replication.

In summary, our data here demonstrate important roles of cholesterol and sphingolipid in HCV infection and virion maturation. Specifically, mature HCV particles are rich in cholesterol. Depletion from HCV or hydrolysis of virion-associated SM results in a loss of infectivity. Moreover, the addition of exogenous cholesterol restores infectivity. In addition, cholesterol and sphingolipid on the HCV membrane play key roles in virus internalization, and portions of structural proteins are localized at lipid-raft-like membrane structures within cells. Finally, inhibitors of the sphingolipid biosynthetic pathway efficiently block virion production. These observations suggest that agents capable of modifying virion-associated lipid content might function as antivirals by preventing and/or blocking HCV infection and production.

ACKNOWLEDGMENTS

We thank M. Matsuda, M. Sasaki, S. Yoshizaki, T. Shimoji, M. Kaga, and T. Date for technical assistance and T. Mizoguchi for secretarial work.

This work was partially supported by a grant-in-aid for Scientific Research from the Japan Society for the Promotion of Science, from the Ministry of Health, Labor, and Welfare of Japan, and from the Ministry of Education, Culture, Sports, Science, and Technology, as well as by a Research on Health Science Focusing on Drug Innovation grant from the Japan Health Sciences Foundation.

REFERENCES

1. **Aizaki, H., Y. Aoki, T. Harada, K. Ishii, T. Suzuki, S. Nagamori, G. Toda, Y. Matsuura, and T. Miyamura.** 1998. Full-length complementary DNA of hepatitis C virus genome from an infectious blood sample. Hepatology **27:** 621–627.
2. **Aizaki, H., K. J. Lee, V. M. Sung, H. Ishiko, and M. M. Lai.** 2004. Characterization of the hepatitis C virus RNA replication complex associated with lipid rafts. Virology **324:**450–461.
3. **Akazawa, D., T. Date, K. Morikawa, A. Murayama, M. Miyamoto, M. Kaga, H. Barth, T. F. Baumert, J. Dubuisson, and T. Wakita.** 2007. CD81 expression is important for the permissiveness of Huh7 cell clones for heterogeneous hepatitis C virus infection. J. Virol. **81:**5036–5045.
4. **Bender, F. C., J. C. Whitbeck, H. Lou, G. H. Cohen, and R. J. Eisenberg.** 2005. Herpes simplex virus glycoprotein B binds to cell surfaces independently of heparan sulfate and blocks virus entry. J. Virol. **79:**11588–11597.
5. **Blanchard, E., D. Brand, S. Trassard, A. Goudeau, and P. Roingeard.** 2002. Hepatitis C virus-like particle morphogenesis. J. Virol. **76:**4073–4079.
6. **Chazal, N., and D. Gerlier.** 2003. Virus entry, assembly, budding, and membrane rafts. Microbiol. Mol. Biol. Rev. **67:**226–237.
7. **Evans, M. J., T. von Hahn, D. M. Tscherne, A. J. Syder, M. Panis, B. Wolk, T. Hatziioannou, J. A. McKeating, P. D. Bieniasz, and C. M. Rice.** 2007. Claudin-1 is a hepatitis C virus co-receptor required for a late step in entry. Nature **446:**801–805.
8. **Ezelle, H. J., D. Markovic, and G. N. Barber.** 2002. Generation of hepatitis C virus-like particles by use of a recombinant vesicular stomatitis virus vector. J. Virol. **76:**12325–12334.
9. **Fukasawa, M., M. Nishijima, H. Itabe, T. Takano, and K. Hanada.** 2000. Reduction of sphingomyelin level without accumulation of ceramide in Chinese hamster ovary cells affects detergent-resistant membrane domains and enhances cellular cholesterol efflux to methyl-β-cyclodextrin. J. Biol. Chem. **275:**34028–34034.
10. **Gao, L., H. Aizaki, J. W. He, and M. M. Lai.** 2004. Interactions between viral nonstructural proteins and host protein hVAP-33 mediate the formation of hepatitis C virus RNA replication complex on lipid raft. J. Virol. **78:**3480–3488.
11. **Guo, J. T., V. V. Bichko, and C. Seeger.** 2001. Effect of alpha interferon on the hepatitis C virus replicon. J. Virol. **75:**8516–8523.
12. **Hanada, K., T. Hara, M. Fukasawa, A. Yamaji, M. Umeda, and M. Nishijima.** 1998. Mammalian cell mutants resistant to a sphingomyelin-directed cytolysin. Genetic and biochemical evidence for complex formation of the LCB1 protein with the LCB2 protein for serine palmitoyltransferase. J. Biol. Chem. **273:**33787–33794.
13. **Hase, T., P. L. Summers, K. H. Eckels, and W. B. Baze.** 1987. An electron and immunoelectron microscopic study of dengue-2 virus infection of cultured mosquito cells: maturation events. Arch. Virol. **92:**273–291.
14. **Heider, J. G., and R. L. Boyett.** 1978. The picomole determination of free and total cholesterol in cells in culture. J. Lipid Res. **19:**514–518.
15. **Heinz, F. X., and S. L. Allison.** 2003. Flavivirus structure and membrane fusion. Adv. Virus Res. **59:**63–97.
16. **Huang, H., F. Sun, D. M. Owen, W. Li, Y. Chen, M. Gale, and J. Ye.** 2007. Hepatitis C virus production by human hepatocytes dependent on assembly and secretion of very low-density lipoproteins. Proc. Natl. Acad. Sci. USA **104:**5848–5853.
17. **Ikeda, M., M. Yi, K. Li, and S. M. Lemon.** 2002. Selectable subgenomic and genome-length dicistronic RNAs derived from an infectious molecular clone of the HCV-N strain of hepatitis C virus replicate efficiently in cultured Huh7 cells. J. Virol. **76:**2997–3006.
18. **Ishii, N., K. Watashi, T. Hishiki, K. Goto, D. Inoue, M. Hijikata, T. Wakita, N. Kato, and K. Shimotohno.** 2006. Diverse effects of cyclosporine on hepatitis C virus strain replication. J. Virol. **80:**4510–4520.
19. **Kapadia, S. B., H. Barth, T. Baumert, J. A. McKeating, and F. V. Chisari.** 2007. Initiation of hepatitis C virus infection is dependent on cholesterol and cooperativity between CD81 and scavenger receptor B type I. J. Virol. **81:**374–383.
20. **Kato, T., A. Furusaka, M. Miyamoto, T. Date, K. Yasui, J. Hiramoto, K. Nagayama, T. Tanaka, and T. Wakita.** 2001. Sequence analysis of hepatitis C virus isolated from a fulminant hepatitis patient. J. Med. Virol. **64:**334–339.
21. **Kato, T., T. Date, M. Miyamoto, A. Furusaka, K. Tokushige, M. Mizokami, and T. Wakita.** 2003. Efficient replication of the genotype 2a hepatitis C virus subgenomic replicon. Gastroenterology **125:**1808–1817.
22. **Kato, T., T. Date, M. Miyamoto, M. Sugiyama, Y. Tanaka, E. Orito, T. Ohno, K. Sugihara, I. Hasegawa, K. Fujiwara, K. Ito, A. Ozasa, M. Mizokami, and T. Wakita.** 2005. Detection of anti-hepatitis C virus effects of interferon and ribavirin by a sensitive replicon system. J. Clin. Microbiol. **43:**5679–5684.
23. **Kato, T., T. Date, A. Murayama, K. Morikawa, D. Akazawa, and T. Wakita.** 2006. Cell culture and infection system for hepatitis C virus. Nat. Protoc. **1:**2334–2339.
24. **Kobayashi, S, K. Kakumoto, and M. Sugiura.** 2002. Transition metal salts-catalyzed aza-Michael reactions of enones with carbamates. Org. Lett. **18:** 1319–1322.
25. **Koutsoudakis, G., E. Herrmann, S. Kallis, R. Bartenschlager, and T. Pietschmann.** 2007. The level of CD81 cell surface expression is a key determinant for productive entry of hepatitis C virus into host cells. J. Virol. **81:**588–598.
26. **Lohmann, V., F. Korner, J. Koch, U. Herian, L. Theilmann, and R. Bartenschlager.** 1999. Replication of subgenomic hepatitis C virus RNAs in a hepatoma cell line. Science **285:**110–113.
27. **Mackenzie, J. M., and E. G. Westaway.** 2001. Assembly and maturation of the flavivirus Kunjin virus appear to occur in the rough endoplasmic reticulum and along the secretory pathway, respectively. J. Virol. **75:**10787–10799.
28. **Manes, S., G. del Real, R. A. Lacalle, P. Lucas, C. Gomez-Mouton, S. Sanchez-Palomino, R. Delgado, J. Alcami, E. Mira, and A. C. Martinez.**

2000. Membrane raft microdomains mediate lateral assemblies required for HIV-1 infection. EMBO 1:190–196.
29. **Matsuo, E., H. Tani, C. Lim, Y. Komoda, T. Okamoto, H. Miyamoto, K. Moriishi, S. Yagi, A. H. Patel, T. Miyamura, and Y. Matsuura.** 2006. Characterization of HCV-like particles produced in a human hepatoma cell line by a recombinant baculovirus. Biochem. Biophys. Res. Commun. **340:**200–208.
30. **Matto, M., C. M. Rice, B. Aroeti, and J. S. Glenn.** 2004. Hepatitis C virus core protein associates with detergent-resistant membranes distinct from classical plasma membrane rafts. J. Virol. **78:**12047–12053.
31. **Miyake, Y., Y. Kozutsumi, S. Nakamura, T. Fujita, and T. Kawasaki.** 1995. Serine palmitoyltransferase is the primary target of a sphingosine-like immunosuppressant, ISP-1/myriocin. Biochem. Biophys. Res. Commun. **211:** 396–403.
32. **Miyanari, Y., K. Atsuzawa, N. Usuda, K. Watashi, T. Hishiki, M. Zayas, R. Bartenschlager, T. Wakita, M. Hijikata, and K. Shimotohno.** 2007. The lipid droplet is an important organelle for hepatitis C virus production. Nat. Cell Biol. **9:**1089–1097.
33. **Morikawa, K., Z. Zhao, T. Date, M. Miyamoto, A. Murayama, D. Akazawa, J. Tanabe, S. Sone, and T. Wakita.** 2007. The roles of CD81 and glycosaminoglycans in the adsorption and uptake of infectious HCV particles. J. Med. Virol. **79:**714–723.
34. **Murakami, K., K. Ishii, Y. Ishihara, S. Yoshizaki, K. Tanaka, Y. Gotoh, H. Aizaki, M. Kohara, H. Yoshioka, Y. Mori, N. Manabe, I. Shoji, T. Sata, R. Bartenschlager, Y. Matsuura, T. Miyamura, and T. Suzuki.** 2006. Production of infectious hepatitis C virus particles in three-dimensional cultures of the cell line carrying the genome-length dicistronic viral RNA of genotype 1b. Virology **351:**381–392.
35. **Nakai, K., T. Okamoto, T. Kimura-Someya, K. Ishii, C. K. Lim, H. Tani, E. Matsuo, T. Abe, Y. Mori, T. Suzuki, T. Miyamura, J. H. Nunberg, K. Moriishi, and Y. Matsuura.** 2006. Oligomerization of hepatitis C virus core protein is crucial for interaction with the cytoplasmic domain of E1 envelope protein. J. Virol. **80:**11265–11273.
36. **Ng, M. L., J. Howe, V. Sreenivasan, and J. J. Mulders.** 1994. Flavivirus West Nile (Sarafend) egress at the plasma membrane. Arch. Virol. **137:**303–313.
37. **Ng, M. L., S. H. Tan, and J. J. Chu.** 2001. Transport and budding at two distinct sites of visible nucleocapsids of West Nile (Sarafend) virus. J. Med. Virol. **65:**758–764.
38. **Niwa, H., K. Yamamura, and J. Miyazaki.** 1991. Efficient selection for high-expression transfectants with a novel eukaryotic vector. Gene **108:**193–199.
39. **Pessin, J. E., and M. Glaser.** 1980. Budding of Rous sarcoma virus and vesicular stomatitis virus from localized lipid regions in the plasma membrane of chicken embryo fibroblasts. J. Biol. Chem. **255:**9044–9050.
40. **Pitha, J., T. Irie, P. B. Sklar, and J. S. Nye.** 1988. Drug solubilizers to aid pharmacologists: amorphous cyclodextrin derivatives. Life Sci. **43:**493–502.
41. **Rahman, S., T. Matsumura, K. Masuda, K. Kanemura, and T. Fukunaga.** 1998. Maturation site of dengue type 2 virus in cultured mosquito C6/36 cells and Vero cells. Kobe J. Med. Sci. **44:**65–79.
42. **Rouser, G., G. Galli, and G. Kritchevsky.** 1967. Lipid composition of the normal human brain and its variations during various diseases. Pathol. Biol. **15:**195–200.
43. **Sakamoto, H., K. Okamoto, M. Aoki, H. Kato, A. Katsume, A. Ohta, T. Tsukuda, N. Shimma, Y. Aoki, M. Arisawa, M. Kohara, and M. Sudoh.** 2005. Host sphingolipid biosynthesis as a target for hepatitis C virus therapy. Nat. Chem. Biol. **1:**333–337.
44. **Sato, K., H. Okamoto, S. Aihara, Y. Hoshi, T. Tanaka, and S. Mishiro.** 1993. Demonstration of sugar moiety on the surface of hepatitis C virions recovered from the circulation of infected humans. Virology **196:**354–357.
45. **Serafino, A., M. B. Valli, F. Andreola, A. Crema, G. Ravagnan, L. Bertolini, and G. Carloni.** 2003. Suggested role of the Golgi apparatus and endoplasmic reticulum for crucial sites of hepatitis C virus replication in human lymphoblastoid cells infected in vitro. J. Med. Virol. **70:**31–41.
46. **Shi, S. T., K. J. Lee, H. Aizaki, S. B. Hwang, and M. M. Lai.** 2003. Hepatitis C virus RNA replication occurs on a detergent-resistant membrane that cofractionates with caveolin-2. J. Virol. **77:**4160–4168.
47. **Shinitzky, M., and M. Inbar.** 1976. Microviscosity parameters and protein mobility in biological membranes. Biochim. Biophys. Acta **433:**133–149.
48. **Shirakura, M., K. Murakami, T. Ichimura, R. Suzuki, T. Shimoji, K. Fukuda, K. Abe, S. Sato, M. Fukasawa, Y. Yamakawa, M. Nishijima, K. Moriishi, Y. Matsuura, T. Wakita, T. Suzuki, P. M. Howley, T. Miyamura, and I. Shoji.** 2007. E6AP ubiquitin ligase mediates ubiquitylation and degradation of hepatitis C virus core protein. J. Virol. **81:**1174–1185.
49. **Stuart, A. D., H. E. Eustace, T. A. McKee, and T. D. Brown.** 2002. A novel cell entry pathway for a DAF-using human enterovirus is dependent on lipid rafts. J. Virol. **76:**9307–9322.
50. **Takikawa, S., K. Ishii, H. Aizaki, T. Suzuki, H. Asakura, Y. Matsuura, and T. Miyamura.** 2000. Cell fusion activity of hepatitis C virus envelope proteins. J. Virol. **74:**5066–5074.
51. **Tani, H., Y. Komoda, E. Matsuo, K. Suzuki, I. Hamamoto, T. Yamashita, K. Moriishi, K. Fujiyama, T. Kanto, N. Hayashi, A. Owsianka, A. H. Patel, M. A. Whitt, and Y. Matsuura.** 2007. Replication-competent recombinant vesicular stomatitis virus encoding hepatitis C virus envelope proteins. J. Virol. **81:**8601–8612.
52. **Umehara, T., M. Sudoh, F. Yasui, C. Matsuda, Y. Hayashi, K. Chayama, and M. Kohara.** 2006. Serine palmitoyltransferase inhibitor suppresses HCV replication in a mouse model. Biochem. Biophys. Res. Commun. **346:**67–73.
53. **Voisset, C., M. Lavie, F. Helle, A. Op De Beeck, A. Bilheu, J. Bertrand-Michel, F. Tercé, L. Cocquerel, C. Wychowski, N. Vu-Dac, and J. Dubuisson.** 2008. Ceramide enrichment of the plasma membrane induces CD81 internalization and inhibits hepatitis C virus entry. Cell. Microbiol. **10:**606–617.
54. **Wakita, T., T. Pietschmann, T. Kato, T. Date, M. Miyamoto, Z. Zhao, K. Murthy, A. Habermann, H. G. Krausslich, M. Mizokami, R. Bartenschlager, and T. J. Liang.** 2005. Production of infectious hepatitis C virus in tissue culture from a cloned viral genome. Nat. Med. **11:**791–796.
55. **Yasuda, S., H. Kitagawa, M. Ueno, H. Ishitani, M. Fukasawa, M. Nishijima, S. Kobayashi, and K. Hanada.** 2001. A novel inhibitor of ceramide trafficking from the endoplasmic reticulum to the site of sphingomyelin synthesis. J. Biol. Chem. **276:**43994–44002.
56. **Zhong, J., P. Gastaminza, G. Cheng, S. Kapadia, T. Kato, D. R. Burton, S. F. Wieland, S. L. Uprichard, T. Wakita, and F. V. Chisari.** 2005. Robust hepatitis C virus infection in vitro. Proc. Natl. Acad. Sci. USA **102:**9294–9299.

Biochemical and Biophysical Research Communications 379 (2009) 330–334

Contents lists available at ScienceDirect

Biochemical and Biophysical Research Communications

journal homepage: www.elsevier.com/locate/ybbrc

3D cultured immortalized human hepatocytes useful to develop drugs for blood-borne HCV

Hussein Hassan Aly [a], Kunitada Shimotohno [b], Makoto Hijikata [a,c,*]

[a] Laboratory of Human Tumor Viruses, The Institute for Virus Research, Kyoto University, Department of Viral Oncology, 53 Kawaharacho, Shogoin, Sakyoku, Kyoto 606-8507, Japan
[b] Center for Human Metabolomic Systems Biology, Keio University, 35 Shinano-machi, Shinjuku-ku, Tokyo 160-8582, Japan
[c] Laboratory of Viral Oncology, Graduate School of Biostudies, Kyoto University, Konoecho, Yoshida, Sakyoku, Kyoto 606-8501, Japan

ARTICLE INFO

Article history:
Received 5 December 2008
Available online 25 December 2008

Keywords:
Hepatitis C virus
Infection
Replication
3D culture
PPAR
Immortalized hepatocytes
Blood-borne HCV

ABSTRACT

Due to the high polymorphism of natural hepatitis C virus (HCV) variants, existing recombinant HCV replication models have failed to be effective in developing effective anti-HCV agents. In the current study, we describe an *in vitro* system that supports the infection and replication of natural HCV from patient blood using an immortalized primary human hepatocyte cell line cultured in a three-dimensional (3D) culture system. Comparison of the gene expression profile of cells cultured in the 3D system to those cultured in the existing 2D system demonstrated an up-regulation of several genes activated by peroxisome proliferator-activated receptor alpha (PPARα) signaling. Furthermore, using PPARα agonists and antagonists, we also analyzed the effect of PPARα signaling on the modulation of HCV replication using this system. The 3D *in vitro* system described in this study provides significant insight into the search for novel anti-HCV strategies that are specific to various strains of HCV.

Infection with Hepatitis C virus (HCV) is a serious health problem worldwide and leads to high rates of liver cirrhosis and hepatocellular carcinoma [1]. Given that the standard HCV therapy remains insufficient for the successful treatment of many patients [2], the development of more effective and less toxic anti-HCV agents is required. *In vitro* systems like the HCV replicon-bearing cells and the infectious particle-producing JFH1 system, has contributed to the discovery of new targets for anti-HCV therapy. However, these recombinant HCV genomes only proliferate in sublines of HuH-7 cells, which do not permit infection or proliferation of blood-borne HCV. Due to the high polymorphism of natural HCV, data from recombinant HCV systems could be evaluated by studying the therapeutic response of a variety of naturally occurring HCVs. However, the current systems available for such study remain insufficient due to the low infection and replication efficiency of the natural HCV strains.

More recently, production and secretion of infectious HCV particles has been reported in two independent three-dimensional (3D) cell culture systems, termed the radial-flow bioreactor (3D/RFB) and the thermoreversible gelatin polymer (3D/TGP) systems. These results were not observed in monolayer cultures [3], suggesting that hepatocytes cultured in 3D more closely resemble liver cells *in vivo* [4] and thus support HCV proliferation. In addition, analysis of gene expression levels in 3D cultured cells revealed that the newly established immortalized human hepatocyte (HuS-E/2 cells) gene profile was altered to more closely resemble that of human liver tissue when the cells were cultured in 3D/TGP [5].

In the current study, we cultured HuS-E/2 cells in 3D/TGP and demonstrated efficient proliferation of natural HCV. Furthermore, gene expression analysis of these cells demonstrated the activation of the peroxisome proliferators-activated receptor α (PPARα) signaling pathway, suggesting an important role for this pathway in the replication of natural HCV. Thus, the *in vitro* system described appears to be a useful tool for the study of HCV infection and proliferation as well as for the development of effective anti-viral agents against various natural HCVs.

Materials and methods

Cell culture. Immortalized human hepatocytes (HuS-E/2) and LucNeo#2 replicon cells [6] were cultured as previously described [5,7]. For the 3D-TGP culture system, 1×10^5 HuS-E/2 cells were cultured in 1 ml Mebiol gel (Mebiol Inc., Kanagawa, Japan)/well in 12-well plates. Five hundred microliters of fresh medium was overlaid on the solidified gel, and was changed every 2 days. Cell

* Corresponding author. Address: Laboratory of Human Tumor Viruses, The Institute for Virus, Kyoto University, Department of Viral Oncology, 53 Kawaharacho, Shogoin, Sakyoku, Kyoto 606-8507, Japan. Fax: +81 75 751 3998.
E-mail address: mhijikat@virus.kyoto-u.ac.jp (M. Hijikata).

0006-291X/$ - see front matter © 2008 Elsevier Inc. All rights reserved.
doi:10.1016/j.bbrc.2008.12.054

extraction from the gel was done at the designated time points according to the manufacturer's protocol.

RNA extraction, reverse transcriptase polymerase chain reaction (RT-PCR) and real-time RT-PCR (Q-PCR). At the designated time points, total cellular RNA was extracted and 1 μg of total RNA was used as a template for RT-PCR and for the quantitative detection of HCV-RNA using real-time RT-PCR (Q-PCR) as previously described [10].

HCV infection experiment. HCV infection experiments were carried out using sera from patients infected with HCV. Infection in 2D culture was undertaken as previously described [5]. For 3D/TGP cultured cells, the gel was solidified, and 50 μl HCV-containing patient serum with a titer of 1×10^6 HCV-RNA/ml was added to the culture and mixed. The culture was continued until the cells were extracted. Following extraction from 3D-TGP, cells were centrifuged and washed three times thoroughly with PBS. RNA was then extracted from the cells as described above. HCV infection into HuS-E/2 cells was also examined in the presence of anti-E2 mouse monoclonal antibody (917) as outlined previously [8].

Treatment of cells with PPARα signaling agonists and antagonists. Fenofibrate or MK886 (Sigma–Aldrich, USA) were added to the culture medium of HuS-E/2 (2D-HuS-E/2) cells from day 0 of HCV infection; or the culture medium of LucNeo#2 replicon harboring cells. The cells were then cultured to the designated time point.

Microarray analysis. Gene expression profiles of 3D/TGP cultured HuS-E/2 cells were obtained by microarray analysis (3D-Genes Human 25, Toray, Tokyo, Japan) and compared to those of cells cultured in 2D.

Results

3D/TGP cultures enhance HCV proliferation in HuS-E/2 cells

Infection and proliferation of the HCV genotype 1b (HCV-RC5) derived from the serum of patient RC5 in HuS-E/2 cells cultured in 3D/TGP (3D/TGP-HuS-E/2 cells) was investigated and compared with that of HuS-E/2 cells cultured in 2D (2D-Hus-E/2). As outlined in Fig. 1A, the HCV-RNA levels in the 3D/TGP-HuS-E/2 cells were significantly higher at all of the time points examined following infection than in the 2D-HuS/E2 cells, suggesting that the 3D/TGP system greatly enhances the proliferation of naturally occurring HCV in HuS-E/2 cells. Similar results were also obtained for sera from additional patients (data not shown). To examine whether the infection is viral envelope-receptor mediated, the infection experiments using serum treated with anti-HCV-E2 antibody (α-E2) or with anti-tubulin (negative control) was also performed. Pre-incubation of the serum with α-E2 significantly reduced the total amount of HCV-RNA in the cells upon infection (Fig. 1B). This result suggested that the infection of natural HCV into 3D/TGP-HuS-E/2 cells was HCV-E2-dependent.

Inhibition of natural HCV replication in HuS-E/2 cells by Interferon

In order to test the effects of anti-viral agents on natural HCV replication in 3D/TGP HuS-E/2 cells, 50–100 U/ml of IFNα was added to the medium overlaying the HCV-RC5 infected 3D/TGP-HuS-E/2 cells. The two treatment concentrations resulted in the inhibition of HCV-RNA replication in 3D-HuS-E/2 cells by

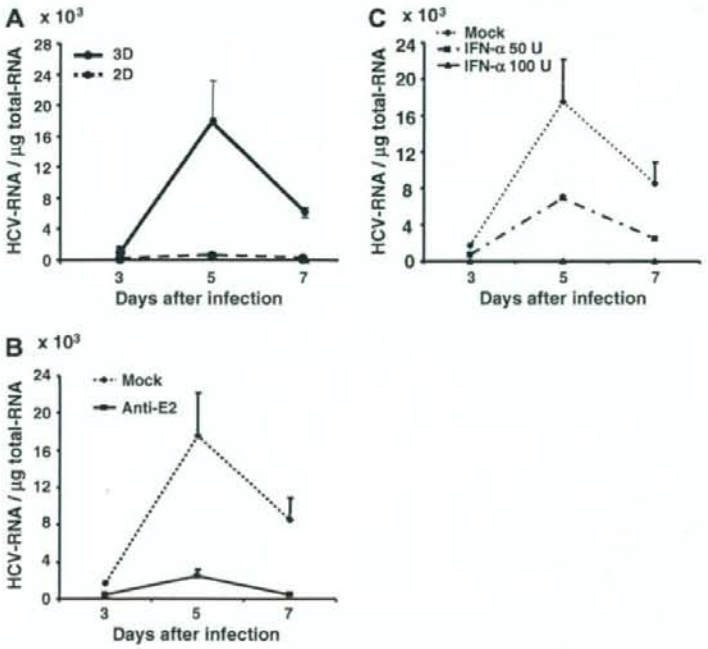

Fig. 1. HCV infection into 3D/TGP-HuS-E/2 cells. (A) 3D/TGP significantly enhanced HCV proliferation in HuS-E/2 cells. HCV patient serum was used to infect a similar number of HuS-E/2 cells cultured in 2D (hashed line) or 3D/TGP (solid line) culture for 24 h. Cells were then harvested and lysed at the indicated time points (3–7 days). The quantity of genomic HCV-RNA per 1 μg total RNA was determined by Q-PCR analysis. (B) Anti-E2 antibodies blocked HCV infection. HCV infection was performed as described in panel A in the presence of Anti-E2 specific or anti-tubulin (control) antibodies. (C) IFNα inhibits HCV replication in 3D/TGP-HuS-E/2 cells. HuS-E/2 cells were infected with HCV and fresh medium supplemented with or without (Mock), 50 U/ml, or 100 U/ml IFNα overlaid on the gel containing the cells and HCV proliferation measured as described above.